

HEAT TRANSFER SIMULATION OF REACTOR CAVITY COOLING SYSTEM  
EXPERIMENTAL FACILITY USING RELAP5-3D AND GENERATION OF VIEW  
FACTORS USING MCNP

A Thesis

by

HUALI WU

Submitted to the Office of Graduate Studies of  
Texas A&M University  
in partial fulfillment of the requirements for the degree of

MASTER OF SCIENCE

Chair of Committee,	Yassin A. Hassan
Co-Chair of Committee,	Sunil S. Chirayath
Committee Members,	Kalyan Annamalai
Head of Department,	Yassan A. Hassan

August 2013

Major Subject: Nuclear Engineering

Copyright 2013 Huali Wu

## ABSTRACT

As one of the most attractive reactor types, The High Temperature Gas-cooled Reactor (HTGR) is designed to be passively safe with the incorporation of Reactor Cavity Cooling System (RCCS). In this paper, a RELAP5-3D simulation model is set up based on the 1/16 scale experimental facility established by Texas A&M University. Also, RELAP5-3D input decks are modified to replicate the experiment procedures and the experimental results are compared with the simulation results. The results show there is a perfect match between experimental and simulation results.

Radiation heat transfer dominates in the heat transfer process of high temperature gas-cooled reactor due to its high operation temperature. According to experimental research done with the RCCS facility in Texas A&M University, radiation heat transfer takes up 80% of the total heat transferred to standing pipes. In radiation heat transfer, the important parameters are view factors between surfaces. However, because of the geometrical complexity in the experimental facility, it is hard to use the numerical method or analytical view factor formula to calculate view factors. In this project, MCNP based on the Monte Carlo method is used to generate view factors for RELAP5-3D input. MCNP is powerful in setting up complicated geometry, source definition and tally application. In the end, RCCS geometry is set up using MCNP and view factors are calculated.

## DEDICATION

To my parents

## ACKNOWLEDGEMENTS

I would like to thank my committee co-chairs, Drs. Hassan and Chirayath, and my committee members, for their guidance and support throughout the course of this research.

Also I would like to thank my friends and colleagues and the department faculty and staff. All of you had made my time at Texas A&M University a great experience. I also want to extend my gratitude to my group members. Thanks for your help and support. It was a great time working with you. Without your kind help, there is no way I can finish this research.

Finally, thanks to my parents and friends for their encouragement and patience and love.

## TABLE OF CONTENTS

	Page
ABSTRACT .....	ii
DEDICATION .....	iii
ACKNOWLEDGEMENTS.....	iv
TABLE OF CONTENTS .....	v
LIST OF FIGURES .....	vii
LIST OF TABLES .....	ix
1 INTRODUCTION .....	1
1.1 Background .....	1
1.1.1 Outline of Reactor Generation .....	1
1.1.2 Description of Gen IV Reactor and RCCS .....	2
1.2 Objectives of Thesis.....	6
2 THERMAL ANALYSIS OF EXPERIMENTAL RCCS WITH RELAP5-3D .....	7
2.1 Description of Experimental Facility.....	7
2.2 Description of RELAP5-3D Model .....	9
2.2.1 Description of RELAP5-3D.....	9
2.2.2 RELAP5-3D Model Setup .....	10
2.3 RCCS Steady State Simulation.....	14
2.3.1 Water Tank as Single Volume Without Secondary Loop.....	14
2.3.2 Water Tank as Pipe with Secondary Loop.....	19
2.3.3 Comparison Between Two Nodalizations .....	23
2.4 Comparison Between RELAP5-3D and Experimental Results.....	25
2.5 Conclusion .....	31
3 GENERATION OF VIEW FACTORS.....	32
3.1 Introduction.....	32
3.2 Methods of View Factor Calculation.....	32
3.3 Validation of View Factor Calculation using MCNP.....	35
3.4 Setup of MCNP Model .....	37
3.5 RCCS View Factor Results.....	41
4 SUMMARY.....	45

REFERENCES.....	46
APPENDIX A.....	48
APPENDIX B.....	49

## LIST OF FIGURES

	Page
Figure 1. Very High Temperature Reactor [2].....	3
Figure 2. Air- Cooled RCCS Conceptual Design .....	4
Figure 3. Water-Cooled RCCS Conceptual Design.....	5
Figure 4. Thermal Fin Concept Design.....	7
Figure 5. Experimental Facility of RCCS system[7] .....	9
Figure 6. Heat Transfer Mechanism[9].....	11
Figure 7. Heat Structure Definition in RELAP5[9] .....	11
Figure 8. Nodalization of RCCS with Boundary Condition .....	13
Figure 9. Cavity Nodalization Top View[9] .....	14
Figure 10. Nodalization of RCCS without Secondary Loop .....	15
Figure 11. Temperature Change in Water Tank (Component 300) .....	16
Figure 12. Mass Flow Rate in Outlet Branch (Component 230-inlet).....	16
Figure 13. Mass Flow Rate in Outlet Branch (Component 230-outlet).....	17
Figure 14. Temperature of Inlet of Outlet Branch .....	17
Figure 15. Temperature of Outlet of Outlet branch .....	18
Figure 16. Temperature of the Inlet of Down-comer.....	18
Figure 17. Temperature of Inlet of the Inlet Branch .....	19
Figure 18. Nodalization of RCCS with Secondary Loop .....	20
Figure 19. Control Variable Variation (006) .....	21
Figure 20. Mass Flow Rate in Outlet Branch .....	22
Figure 21. Mass Flow Rate in Down-comer (core inlet) .....	22
Figure 22. Secondary Loop Mass Flow Rate.....	23
Figure 23. Primary Loop Mass Flow Rate.....	24
Figure 24. Pipe Inlet Temperature .....	24
Figure 25. Pipe Outlet Temperature.....	25
Figure 26. Nodalization for Experiment Configuration.....	26

Figure 27. Secondary Coolant Inlet Temperature in Experiment .....	27
Figure 28. Comparison Between Experiment and RELAP5 .....	28
Figure 29. Power Distribution Over Time (Vessel).....	29
Figure 30. Cavity Outlet Temperature .....	30
Figure 31. Cavity Inlet Temperature.....	30
Figure 32. Primary Loop Mass Flow Rate.....	31
Figure 33. View Factors Between Surfaces of Area $dA_i$ and $dA_j$ [12].....	33
Figure 34. xy Plane View of The Example.....	36
Figure 35. xz Plane View of The Example .....	36
Figure 36. Geometry of Two Infinite Cylinders (3D).....	37
Figure 37. Geometry of Two Infinite Cylinders (XY plane) .....	37
Figure 38. XZ Plane View in MCNP Model .....	38
Figure 39. An Example of Pipe 1 Partition.....	39
Figure 40. XY Plane View in MCNP Model.....	39
Figure 41. Description of Fin Surface Source .....	42
Figure 42. Description of Cylindrical Source .....	43

## LIST OF TABLES

	Page
Table 1. View Factors of Vessel-1 .....	42
Table 2. View Factor of Part a of pipe 1 .....	44
Table 3. Source Surface of P1-Part b .....	49
Table 4. Source Surface of P1-Part c .....	49
Table 5. Source Surface of P2-Part a .....	50
Table 6. Source Surface of P2-Part2 .....	50
Table 7. Source Surface of P2-Part3 .....	51
Table 8. Source Surface of P3-Part a .....	51
Table 9. Source Surface of P3-Part b .....	52
Table 10. Source Surface of P3-Part c .....	52
Table 11. Source Surface of P4-Part a .....	53
Table 12. Source Surface of P4-Part b .....	53
Table 13. Source Surface of P5-Part a .....	54
Table 14. Source Surface of P5-Part b .....	54
Table 15. Source Surface of P5-Part c .....	55
Table 16. Source Surface of P6-Part a .....	55
Table 17. Source Surface of P6-Part b .....	56
Table 18. Source Surface of P7-Part a .....	56
Table 19. Source Surface of P7-Part b .....	57
Table 20. Source Surface of P7-Part c .....	57
Table 21. Source Surface of P8-Part a .....	58
Table 22. Source Surface of P8-Part b .....	58
Table 23. Source Surface of P8-Part c .....	59
Table 24. Source Surface of P9-Part a .....	59
Table 25. Source Surface of P9-Part b .....	60
Table 26. Source Surface of P9-Part c .....	60

# 1 INTRODUCTION

## 1.1 Background

### 1.1.1 Outline of Reactor Generation

There are totally 4 generations of nuclear reactors since the development of nuclear energy--Generation I, II, III, III+, and IV. In general, there exist 6 key reactor attributes[1], which is the main characteristic lies in development and deployment of reactors and reveals the important difference from generation to generation. The first attribute is cost-effectiveness, which makes nuclear energy economically competitive among all energy resources. With better cost-effectiveness, nuclear energy becomes more competitive among all energy resources. The second one is safety. Safety operation of nuclear power plant is always the main concerns when new reactor design is proposed, and passive design feature other than active safety system becomes more and more important in nuclear design, especially after Fukushima reactor accident in 2011. The third one is security and nonproliferation, which addresses the intention to minimize the risks of nuclear theft and terrorism all over the world. The fourth one is grid appropriateness. The first application for most reactors is to produce electricity, so it is essential to make sure the capability of match between local or national electric grid and the electric power a reactor can direct. The fifth one is commercialization roadmap, which must include a perfect timeline for reactor deployment. The sixth one is fuel cycle, which is a critical point in determining risk levels of nuclear safety, security and surety. Front end and back end fuel cycle is two popular types of fuel cycle right now. Based on the six attributes, reactor generations are described as the following: Gen I refers to the prototype and power reactors which consists of early prototype reactors from 1950s and 1960s. Gen II includes many commercial reactors, which is designed to be more economical and reliable with a general operation time of 40 years. The reactor type in Gen II is pressurized water reactor (PWR), CANDU, boiling water reactor (BWR), advanced gas-cooled reactor (AGR) and VVER. Most of operating reactors throughout the world is Gen II, and typical active safety systems related to electrical or mechanical operations are incorporated into design, which can both be initiated manually or automatically. Gen III nuclear reactors are evolved from Gen II with state-of-the-art

design improvement, which mainly reflects in fuel technology, thermal efficiency improvement, modularized constructions, passive safety system design as well as standardized design. The operation life of Gen III is about 60 years, longer than the former generation. The reactor type of Gen III has Westinghouse 600 MW advanced PWR (AP600), Advanced Boiling Water Reactor (ABWR) as well as AP1000 – evolved from AP600. Gen III+ reactor designs are an evolutionary development of Gen III reactors, offering significant improvements in safety over Gen III reactor designs. The most outlining improvement of Gen III+ is the passive safety features independent of active controls or operator intervention but rely on gravity or natural convection to protect the integral of reactor core during abnormal operation. Also, Gen III+ can reach higher fuel burn-up compared to former generations.

### **1.1.2 Description of Gen IV Reactor and RCCS**

The next generation of nuclear power reactors, known as Generation IV reactors, is promised to be much safer and less water intensive, like Gas-cooled fast reactor, Lead-cooled fast reactor, molten salt reactors, sodium-cooled fast reactors, and high temperature gas-cooled reactors. These features make the location of the reactor more flexible. Among all the new concept designs, High Temperature Gas-cooled Reactor (HTGR) is one of the most attracting reactor designs (as shown in Figure 1). It is an inherently safe, graphite-moderated, helium cooled thermal reactor operating under high pressure and high core exit temperature (around 900 °C to 1000 °C). The high coolant exit temperature makes this reactor amenable for some process heat applications such as hydrogen production, district heating as well as potable water production and so on. Also, the reactor efficiency of HTGR can be improved from 33% to almost 50%, which is a major improvement of Generation IV reactors compared to the former generations. Helium, acting as coolant, has attracting advantages over water due to its high incombustible temperature, relatively high specific heat. Moreover, Helium is inert gas, which makes it not radioactive or reacts with materials inside reactor.

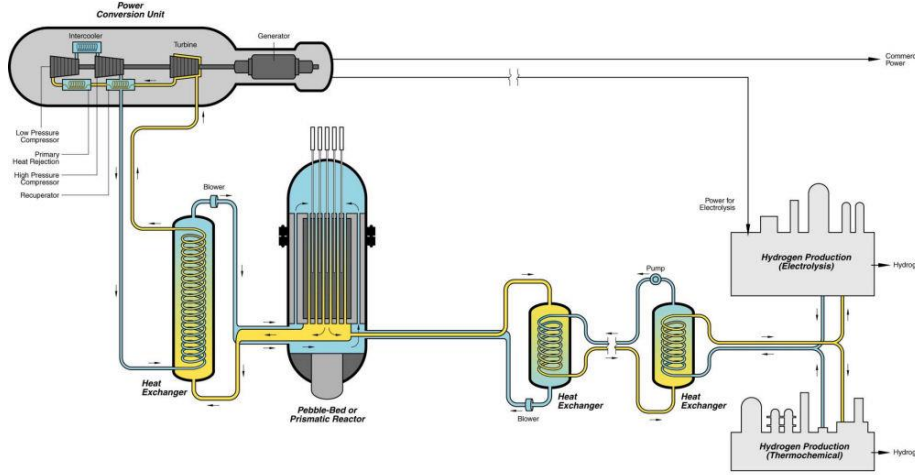


**Figure 1.** Very High Temperature Reactor [2]

As discussed above, HTGR normally operates under harsh environment (high operating pressure and temperature), which challenges the selection of structural materials and behavior of fuel material a lot. The same with other Generation IV reactor designs, HTGR is also designed to be capable of passive safe operations during off-normal and emergency condition and the representing feature is Reactor Cavity Cooling System (RCCS).

RCCS is a heat removal system designed to remove heat that is convected and radiated from the Reactor Pressure Vessel (RPV) wall so the temperature of the structure, cavity wall and fuel can be maintained under acceptable design limit during both normal and off-normal scenarios. RCCS forms a passive heat sink external to the reactor, and is located within the reactor cavity surrounding the metal reactor vessel. During emergency or accident conditions when forced circulation is lost, natural convection of RCCS coolant facilitated by gravity and buoyance removes heat radiated or naturally transferred from the metal vessel to the inner boundary of RCCS facing the vessel by convection. So RCCS will be a first-of-a-kind passive safety system for core decay heat removal[3].

There are two different kinds of RCCS designs based on the working fluid—Air-cooled RCCS[4] and Water-cooled RCCS. The Air-cooled RCCS (as shown in Figure 2)[5], which is proposed by General Atomic, applies cold air as the medium to remove residual heat from reactor cavity. Cold air at atmospheric temperature enters the RCCS from the

top the reactor cavity through inlet duct, and then flows downward via the cooling panel under gravity all the way to the reactor bottom plenum, and finally the air collects heat both radiated and convected from the vessel as it flows through the inner riser pipes. The buoyancy acts as the driven force to move the air to the top of the cavity via the risers. The atmosphere is the ultimate heat sink for air-cooled RCCS.

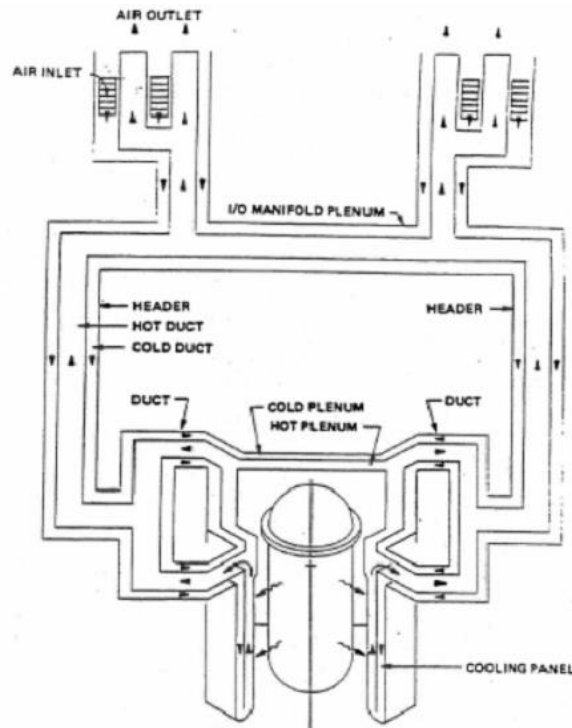


**Figure 2.** Air- Cooled RCCS Conceptual Design

Water-cooled RCCS is proposed by AREVA (as shown in Figure 3)[2] in which water is used to collect heat from reactor cavity also by natural circulation under gravity. Water flows through the cooling panel and moves upward via the riser pipes to a water tank at the top of the reactor. Water-cooled RCCS is also a low-temperature and low-pressure system with the inlet water temperature below 30°C. In normal situation, the water temperature remains unboiling in forced circulation, while during accident scenarios, water will reach boiling commerce and can operate in passive mode for approximately 72 hours. During normal operation, the ultimate heat sink is the secondary heat removal

system. In emergency situation, the heat removed by water natural circulation will be released into the atmosphere by evaporation.

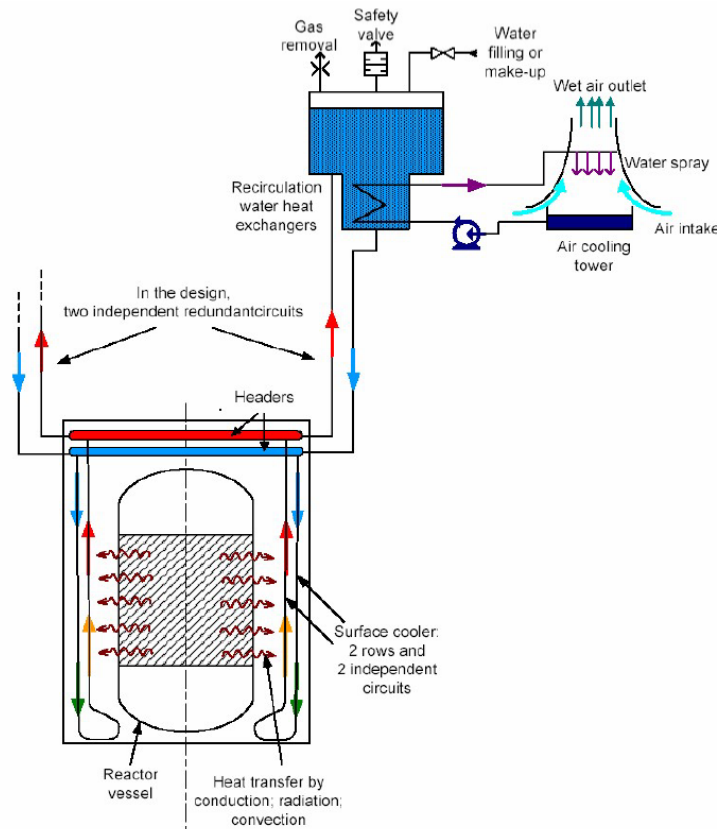


**Figure 3.** Water-Cooled RCCS Conceptual Design

In both water-cooled and air cooled RCCS, part of heat generated inside reactor core will be lost into the reactor cavity by conduction through reactor vessel wall, convection between vessel wall and coolant and radiation within vessel outer surface and the riser pipes' surfaces. Then the coolant inside the risers is heated and the density difference between the heated coolant and the inlet coolant acts as the driven force for natural circulation, which is very important especially in accident scenarios. Overall, both configurations are designed to effectively remove heat from reactor core to maintain fuel integrity as well as structural temperature under design limit no matter what operation conditions the reactor is under.

## **1.2 Objectives of Thesis**

The objective of the thesis is to explore the application of RELAP5-3D in RCCS thermal hydraulic behavior analysis based on small-scale water-cooled experimental facility established by Department of Nuclear Engineering, Texas A&M University. Due to the importance of radiation heat transfer in HTGR, in the thesis, generation of view factors based on RCCS experimental facility using MCNP is also discussed. Finally, it turns out that MCNP is a good way to calculate view factor for irregular and complex system geometry.

## 2 THERMAL ANALYSIS OF EXPERIMENTAL RCCS WITH RELAP5-3D

### 2.1 Description of Experimental Facility

In this thesis, water-cooled RCCS is studied and all research models are based on RCCS experimental facility built by the Texas A&M University.

In RCCS conceptual design, 227 standing pipes are fixed to the cavity walls with supports, surrounding the Reactor Pressurized Vessel (RPV). A typical Water-cooled RCCS conceptual design incorporates thermal-fin concept design (as shown in Figure 4). As shown in the Figure, in thermal-fin design, pipes are connected with thin metal panels welded along the mid-plane of the pipes. 8 water tanks are placed on top of the cavity providing cold coolant to RCCS during normal (forced convection) or off-normal condition (natural convection).

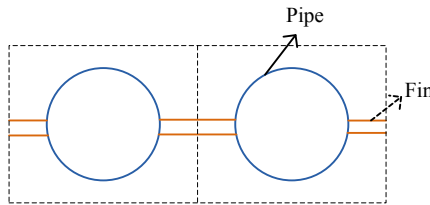


**Figure 4.** Thermal Fin Concept Design

The Texas A&M University experimental facility is a 1/16-scale model[6], which contains 9 standing pipes and a water tank. The experimental facility represents one cooling panel of RCCS system with nine pipes in the cavity, return and supply manifolds connecting standing pipes with water tank and a cylindrical water tank situated at top of the cavity (as shown in Figure 5). In the facility, the cylindrical reactor vessel is approximately treated as a flat surface. Nine risers are thermally connected by a thin metal panel, which is welded along the mid-plane (thermal-fin design). The water tank located on the top of cavity is the ultimate heat sink for the experimental facility system

and water will passively flow downwards under gravity. In the facility, three electrical radiant heaters were installed inside the vessel, which serves as the heat resource for the system. During the experiment, water drawn from the tank flows downward through down-comer under gravity and is collected by the supply manifold, and then cold water is heated inside the pipes by conduction, convection and radiation heat transfer. Water density changes when it is heated towards saturation, and density difference between the inlet cold water and heated water is also the driven force in natural circulation. Hot water coming from the pipes is then collected by top manifold and flows back to the water tank. The water is removed from the tank and passes through a copper coil placed inside an ice storage tank located at the bottom of facility. Cold water is pumped back into the tank through a speed pump. And the injected cold water is sprayed from the top of the tank, so in this case cold water can mix more uniformly with hot water in the tank. In the final configuration, for the secondary loop, the ice melted inside the ice tank acts as the ultimate heat sink for the system. In the experimental facility, the whole pipelines from and to the water tank as well as the reactor vessel are insulated from the outside.

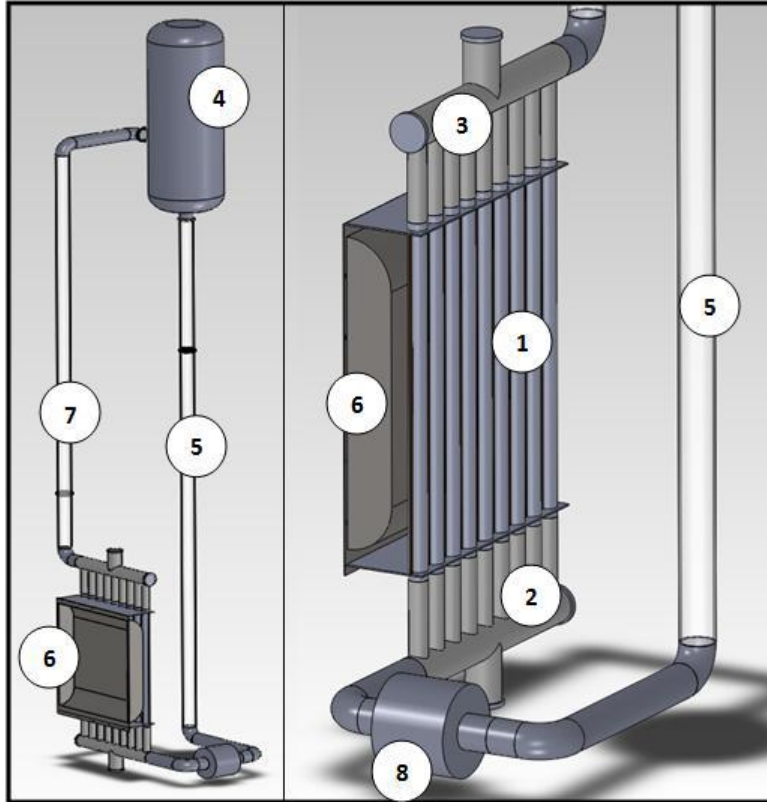


Figure 5. Experimental Facility of RCCS system[7]

## 2.2 Description of RELAP5-3D Model

### 2.2.1 Description of RELAP5-3D

RELAP5-3D code is a thermal hydraulics analysis code, which is specialized for transient analysis like postulated large or small break loss-of-coolant (LOCAs) in light water reactors at first, and it is proven to be powerful in a lot of thermal-hydraulic applications as development continued. Now, it can also be applied to operational transients analysis in PWR as well as Boiling Water Reactor (BWR) system analysis[8]. Equations used in RELAP5-3D incorporate non-equilibrium, nonhomogeneous, six-equation representation, making it possible for two-fluid system simulation for both one-dimensional and multi-dimensional model. In neutronics simulation, the code also has point-kinetics and multi-dimensional nodal neutron kinetics model. Field equations coupled to physics models allow feedback between thermal-hydraulic and neutronics. Moreover, control systems and component models permit simulation of equipment controllers, balance-of-plant

equipment (turbines, pipes), and lumped-node representations of various processes (heat transfer from one volume to another).

The model is composed of hydraulic control volumes, which is connected by either single junction or time-dependent junction and heat structures. In volume definition, besides geometry parameters (volume, flow length and flow area), initial thermal parameters (pressure, temperature, quality and so on) are also defined. Time-dependent volumes and junctions are in charge of specifying boundary conditions. A user-defined property table or control variable can be defined, so the working fluid in the model can either lost in the atmosphere or a system that is not modeled. Given mass flow rate can be given in time-dependent junction to simulate injections or suction. Heat structure defined in RELAP5 can be rectangular, cylindrical or spherical. User-defined tables give the thermal properties of the heat structure. Heat can be transferred to volumes or other heat structures by radiation or conduction by defining either radiation or conduction enclosure. For radiation enclosure, view factors are the input and for conduction enclosure, conduction areas between heat structures are needed.

### **2.2.2 RELAP5-3D Model Setup**

From the above description of RCCS experimental facility, it can be known that heat transfer mechanism in RCCS can be depicted into the following three parts: the first part is radiation heat transfer from RPV to standing pipes; the second part is convection between cavity and standpipes together with fin through air, also convection between pipe inside wall to working fluid inside pipe; the third part is the conduction in fin and pipe walls. However, in RELAP5-3D, only one enclosure can be defined for one case. Experimental work done by R. Vaghetto in TAMU RCCS facility proved that radiation heat transfer dominates in RCCS, indicating almost 80% of the total heat transferred to the standing pipes. Figure 6 and Figure 7 illustrates this heat transfer mechanism and also heat structure definition in RELAP5.

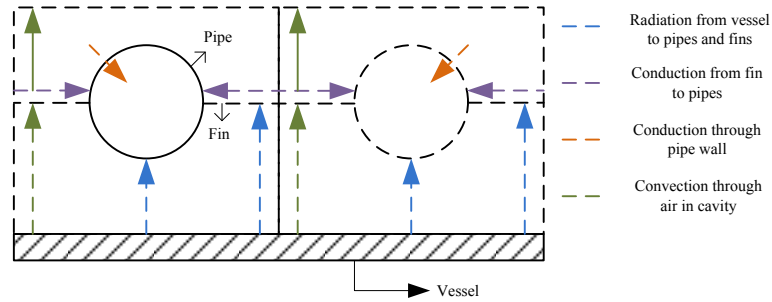


**Figure 6.** Heat Transfer Mechanism[9]

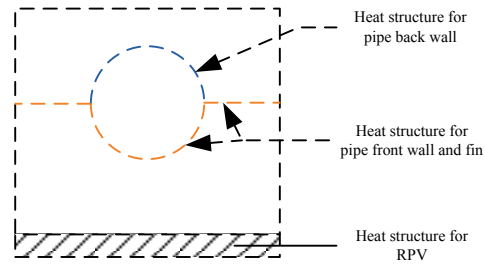


**Figure 7.** Heat Structure Definition in RELAP5[9]

Based on TAMU small-scale experimental facility and the heat transfer theory discussed, a simulation model is set up by RELAP5-3D to analyze the steady-state performance of RCCS. The nodalization is shown in Figure 8 (heat structure is not shown in the nodalization).

In the nodalization, pipe component 300 (divided into 10 sub-volumes) represents water storage tank located at the top of cavity, in which part of the space is air and part of space is water; three branch components 240, 245, 250 represents the inlet pipelines from water tank to the risers; pipe 225, pipe 226 and pipe 227 are return manifolds collecting heated water to water tank; the manifolds are connected via three multiple junction 220, 221, and 222; pipe 255 represents the supply manifold that directs cold water from water tank to 9 standing pipes. Nine pipe components (from 201 to 209), which are divided into five sub-volumes, represent the nine risers in RCCS experimental facility. Time-dependent volume 310 defines the ambient boundary condition about the second loop and allows

heat or vapor discharge to the atmosphere during transient condition. The dimension of all components is also shown in the nodalization. To enable RELAP5 input file to execute without mistake, the dimension shown in the nodalization should make the model a closed loop.

Figure 8 shows general RELAP5 nodalization for RCCS, in the following discussion, several changes are made to this nodalization, which aims at making the simulation model better replicate the experimental facility.

As mentioned above, radiation heat transfer enclosure is defined in RELAP5. So radiation view factors between all heat structures are calculated by NEVADA also by R. Veghato, Texas A&M University. In the second part of the thesis, due to the complexity of geometry (taking into account the axial temperature difference in standing pipes), New view factors are generated using MCNP for RELAP5 input file.

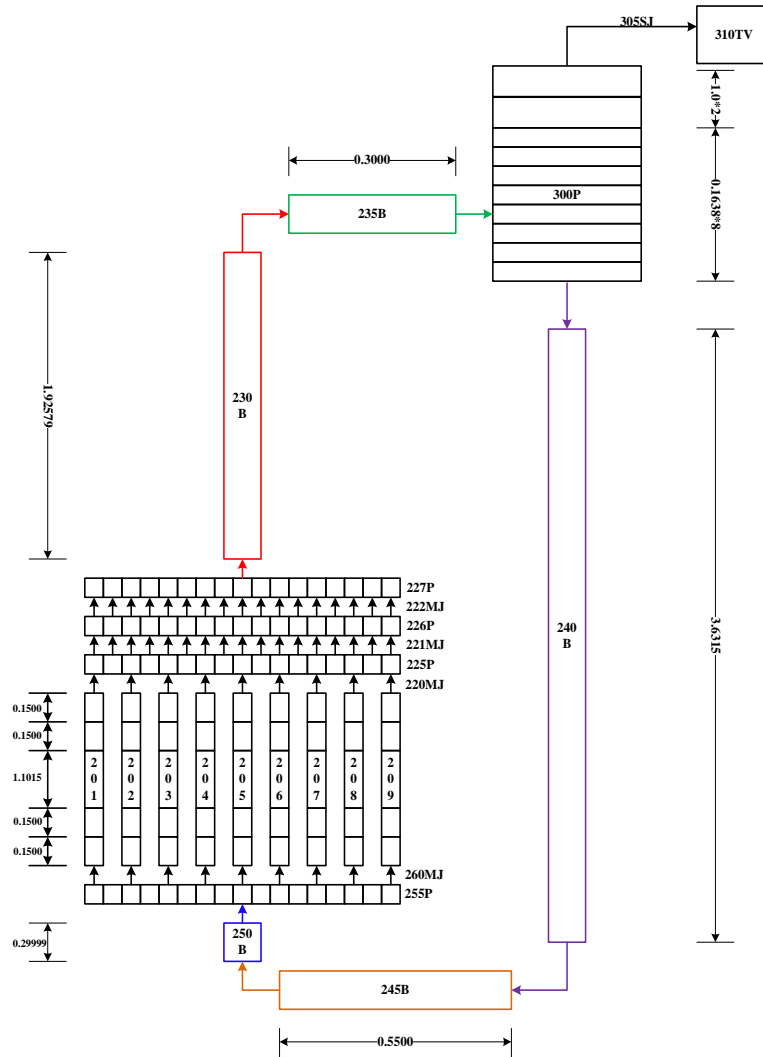


**Figure 8.** Nodalization of RCCS with Boundary Condition

The nodalization of the experimental facility also accounts for heat exchanges between the reactor vessel and pipes as well as heat losses to the environment. As shown in Figure 9, two single volumes filled with air (single volume 100 and 400) are used to model the back and front cavity. And they are connected to a time-dependent volume to maintain the constant atmospheric pressure and temperature.

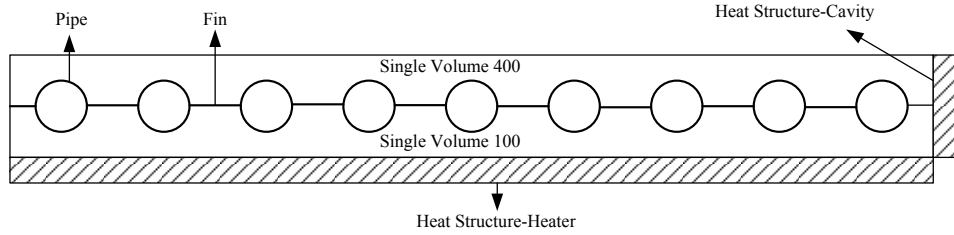


**Figure 9.** Cavity Nodalization Top View[9]

### 2.3 RCCS Steady State Simulation

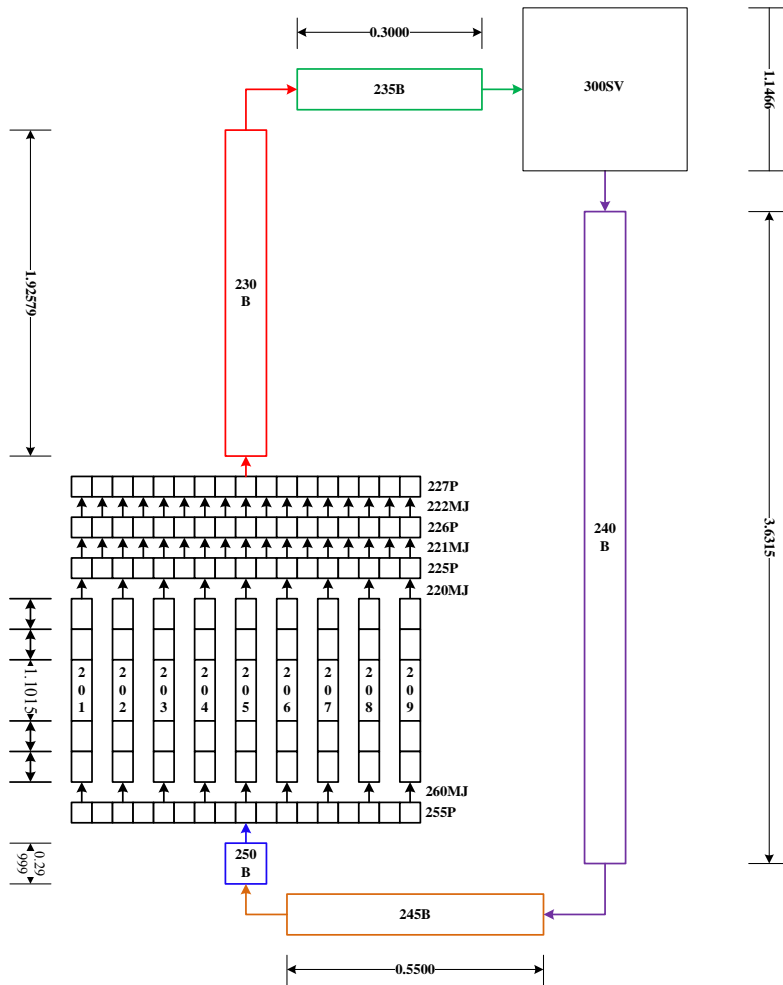
As the system reaches steady state, the power supplied to the system should be equal to the heat removed from the system. In this case, temperature difference between inlet and outlet, total system mass flow rate should be constant.

In this paper, we investigated two different models to remove heat from the system, which can make the system reach a steady state. The difference between the two nodalizations lies in the model of the tank as well as whether the secondary loop is included.

For the first model, the tank is treated as a single volume and there is no secondary loop. Heat structure added to the single volume (tank 300) is used to remove the heat released into the water tank. By adjusting power profile added to the heat structure of the tank, the heat supplied to the system will be removed, and the system will reach steady state when the heat supplied to the system equals to heat removed by heat structure. While in the second model, water tank is simulated by PIPE divided into 10 volumes with both air and water spaces and partial secondary loop is also included. In this case, time-dependent volume and time-dependent junction are used to maintain the boundary condition of water tank (300).

#### 2.3.1 Water Tank as Single Volume Without Secondary Loop

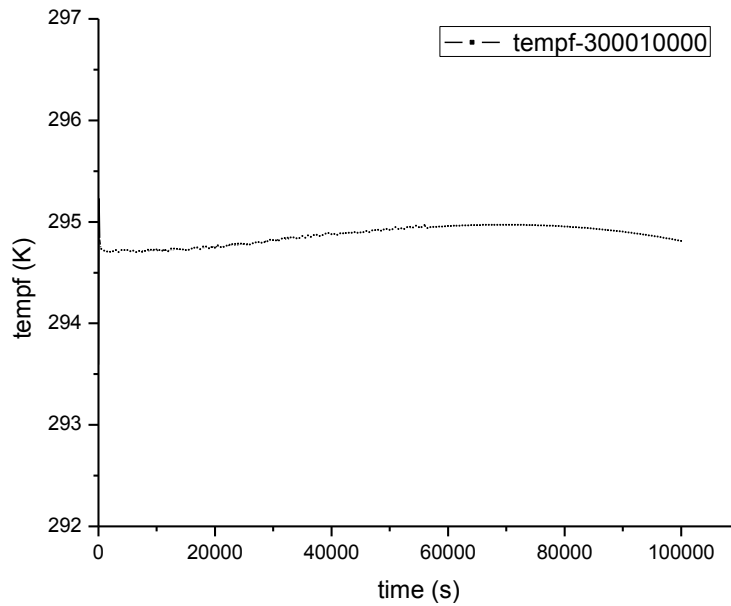
Figure 10 gives the nodalization for the first model.



**Figure 10.** Nodalization of RCCS without Secondary Loop

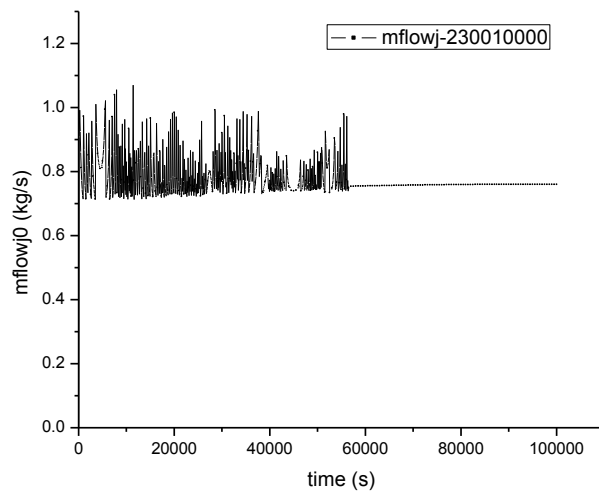
In this model, the water tank is treated as a single volume. In this situation, heat collected by the water is removed by heat structure attached to the water tank component. And the power added to heat structure of the tank was varied with time to make the system reach steady state.

Figure 11 shows the temperature change in water tank with the final power distribution for the tank heat structure. From the figure, we can see the temperature in the tank remains almost constant with very little oscillation (within  $0.5^{\circ}\text{C}$ ), which means by removing the heat in the system by changing the power of the heat structure can make the system reach steady-state.



**Figure 11.** Temperature Change in Water Tank (Component 300)

Other major parameters in the system are also shown in Figures following. System primary mass flow rate is shown in Figure 12 and Figure 13. It shows that after around 5800 s, mass flow rate in outlet branch reaches to a constant value, which means the system is now in steady state.



**Figure 12.** Mass Flow Rate in Outlet Branch (Component 230-inlet)

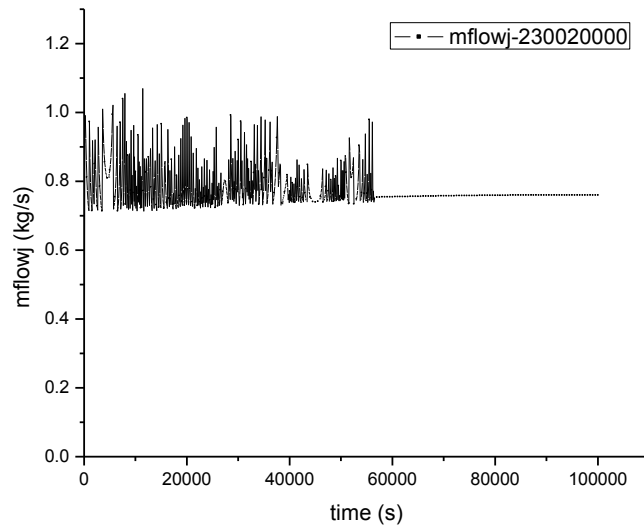


**Figure 13.** Mass Flow Rate in Outlet Branch (Component 230-outlet)

In the following Figure 14 to Figure 17, it shows that after about 58000s, the temperature of down-comer component, outlet branch and inlet branch in the system reaches constant.

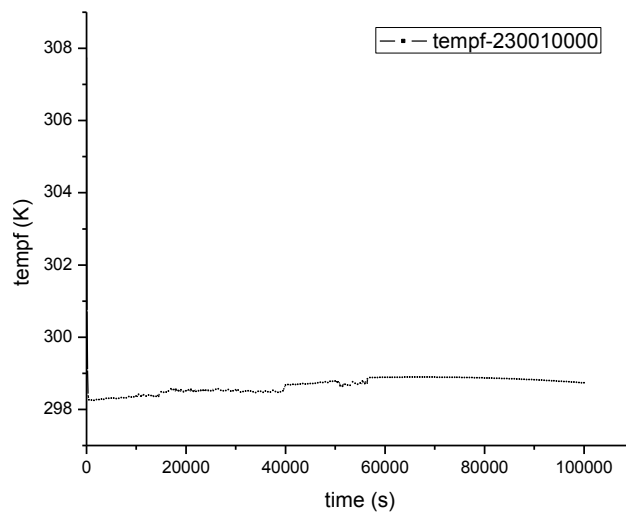


**Figure 14.** Temperature of Inlet of Outlet Branch

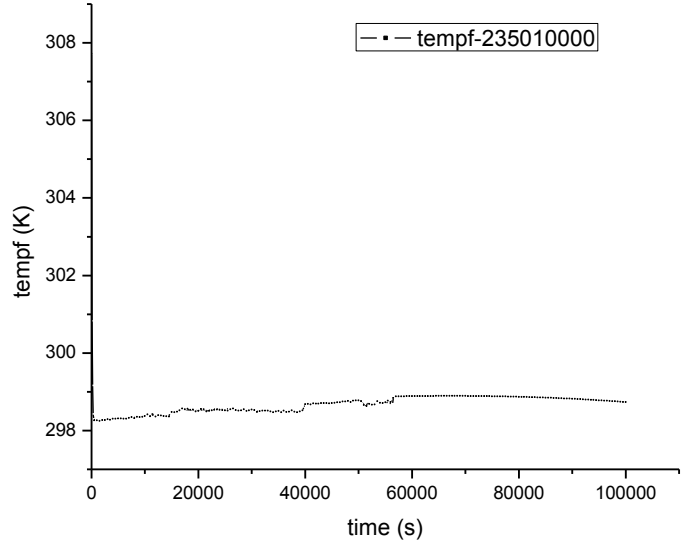


Figure 15. Temperature of Outlet of Outlet branch

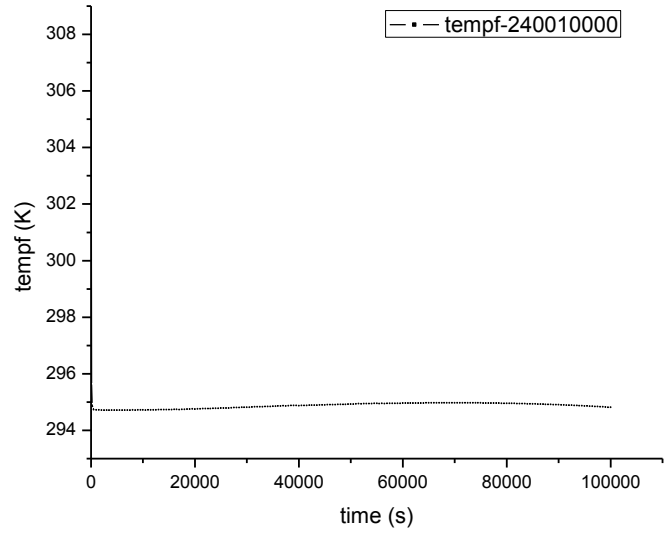
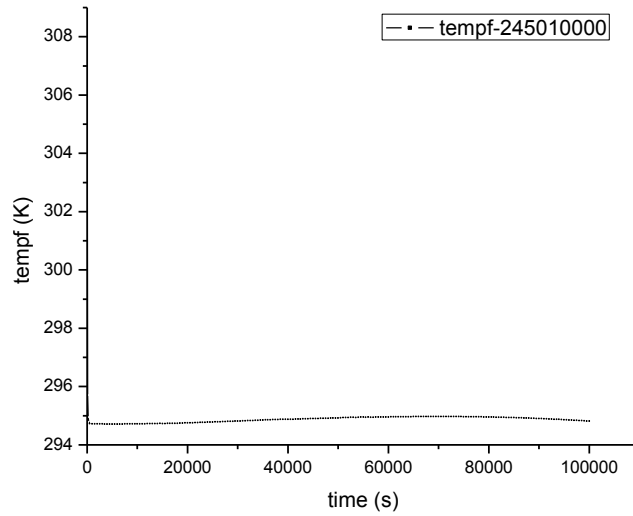


Figure 16. Temperature of the Inlet of Down-comer



**Figure 17.** Temperature of Inlet of the Inlet Branch

### 2.3.2 Water Tank as Pipe with Secondary Loop

The second method applied in the simulation to reach steady state is to treat the water tank as pipes with water and air room and also add secondary loop to the system. The secondary loop contains a time-dependent junction 305 to control the amount of water injected into water tank by control variable. The control variable changes as the difference between the water temperature in the tank and the reference temperature changes. The nodalization for this model is shown in Figure 18.

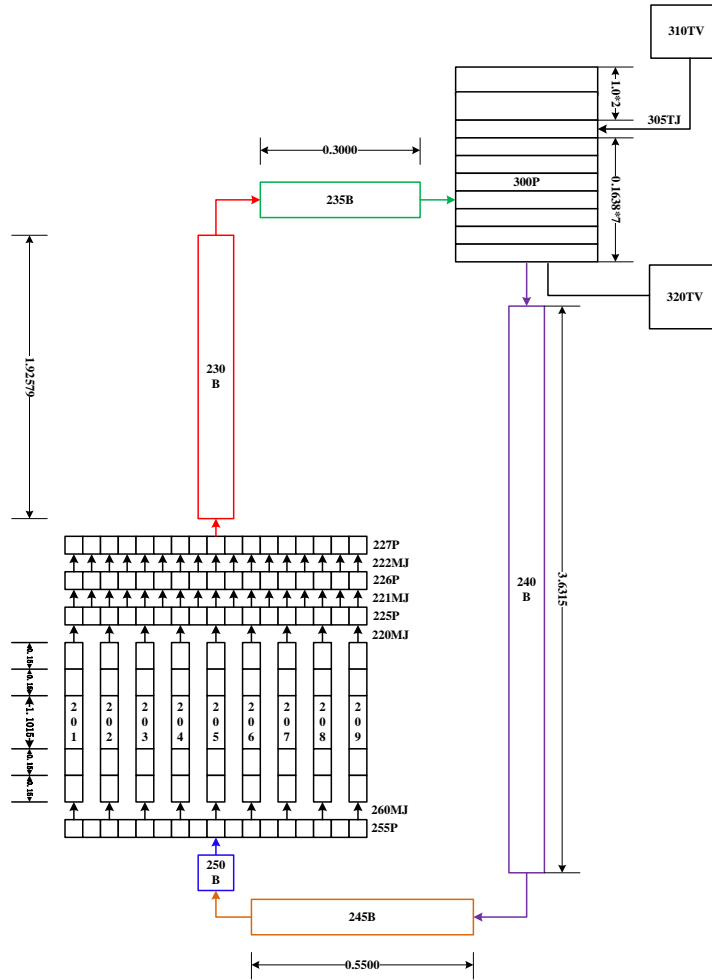


**Figure 18.** Nodalization of RCCS with Secondary Loop

In this nodalization, no heat structure is added to water tank. Instead, a secondary loop with time-dependent volume connected to the inlet and outlet of the tank is applied. A control variable 006 (the temperature difference between the temperature we expected and the temperature calculated in 305) is used to control water injection from time-dependent volume 310 to water tank 300. In this paper, we assume that temperature error between (-1, +1) is acceptable ( $\pm 1$  error is normal in experiment). Figure 19 gives control variable variation during the simulation time (10000s is simulated).

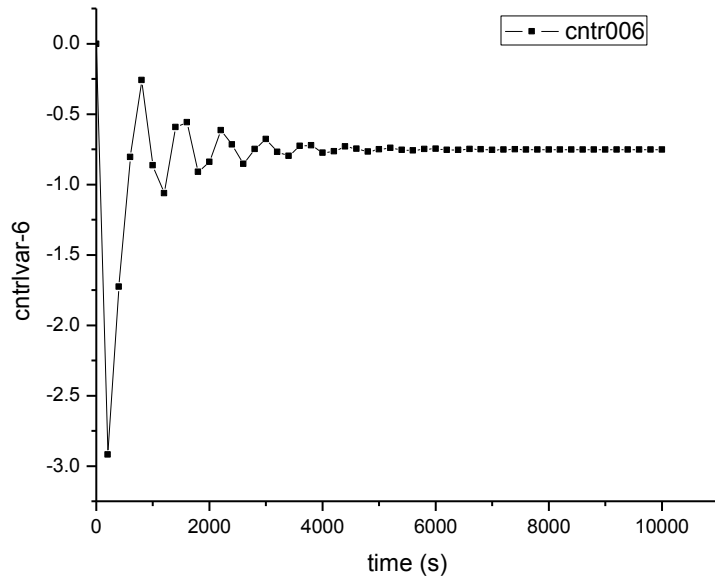


**Figure 19.** Control Variable Variation (006)

In Figure 20, the outlet mass flow rate reaches constant at about 4000s, and the inlet mass flow rate shows the same trend. From the Figure 21, the steady state mass flow rate is approximately 0.8 Kg/s, which is almost the same to the first method to reach steady state. It means both methods can lead the system to steady state, and taking into account the experimental procedure; the second method is used in the following research.

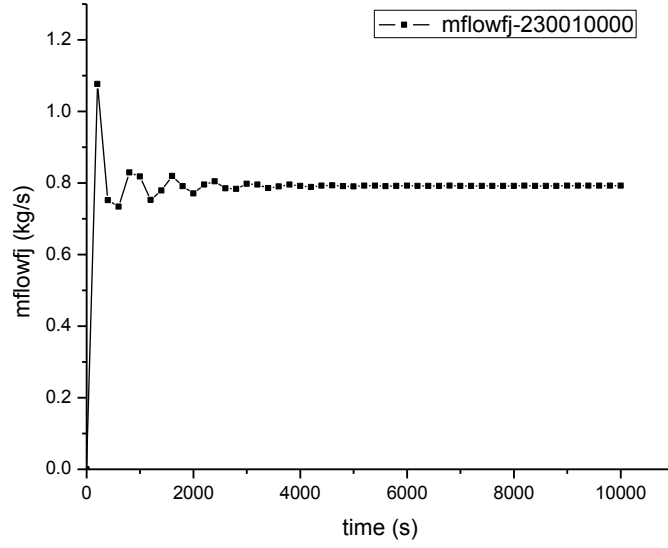


Figure 20. Mass Flow Rate in Outlet Branch

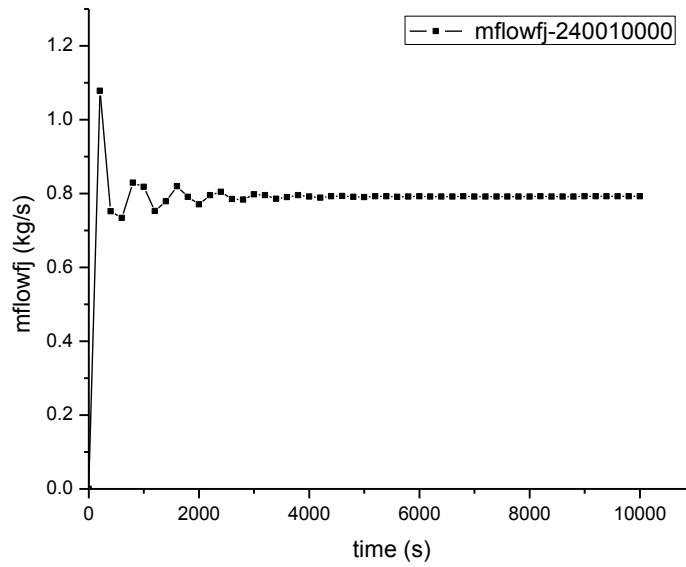


Figure 21. Mass Flow Rate in Down-comer (core inlet)

### 2.3.3 Comparison Between Two Nodalizations

In this section, simulation results from two different nodalizations are compared. Moreover, a 3-D dimensional component defined as MULTID is applied for water tank. MULTID defines three-dimensional array of volumes and the internal junctions connecting the volumes. In Multi-Dimensional Information card CCC0001, it gives the general information about the component like number of intervals for each coordinate, control flag for velocity or mass flow rate, and so on. Among all basic information, the most attracting one is the “three-dimensional flag”, which defines what kind of momentum equations will be used in the 3-dimensional calculations. There are two options: 0 or 1. If the flag is missing or to be set as 0, the three dimensional momentum equations are used; on the contrary, if 1 is defined, one-dimensional momentum equations are used on each of the coordinate directions. Calculations have been done with two options and results are shown in the following figures.

Figure 22 and Figure 23 show the mass flow rate for the primary and secondary loop. For 3-D component, 3-D dimensional flag doesn't make big difference in the mass flow rate, and single volume component matches better with 3-D component than pipe component.

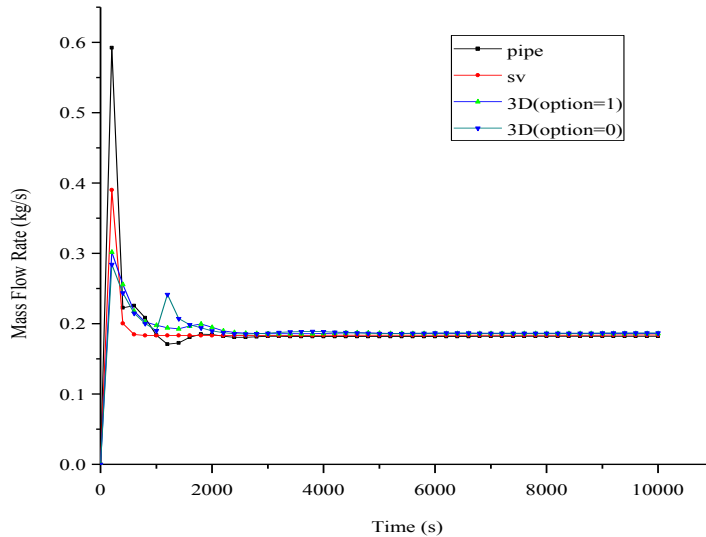
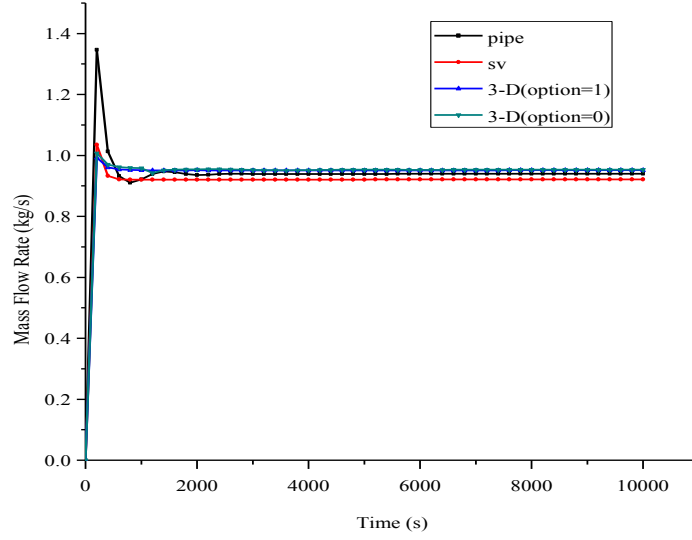
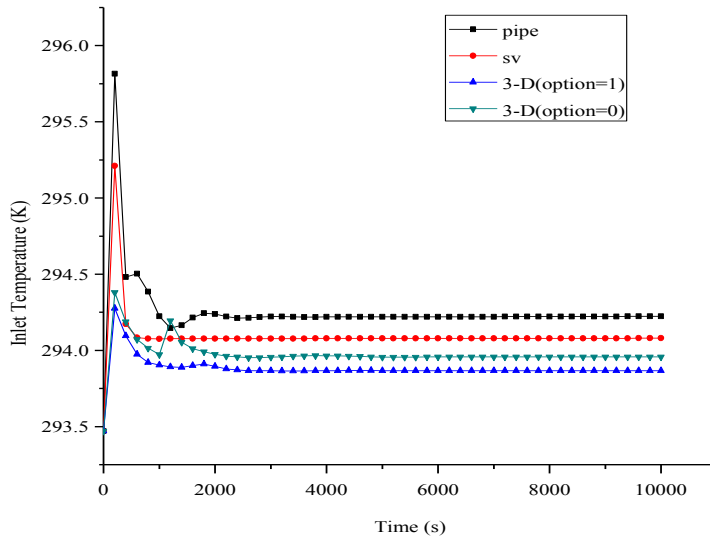


Figure 22. Secondary Loop Mass Flow Rate



**Figure 23.** Primary Loop Mass Flow Rate

Figure 24 and Figure 25 give the pipe inlet and outlet temperature variation. It shows that in 3-D simulation, 3-dimensional momentum equations (flag=0) are better than 1-dimensional momentum equations (flag=1).



**Figure 24.** Pipe Inlet Temperature

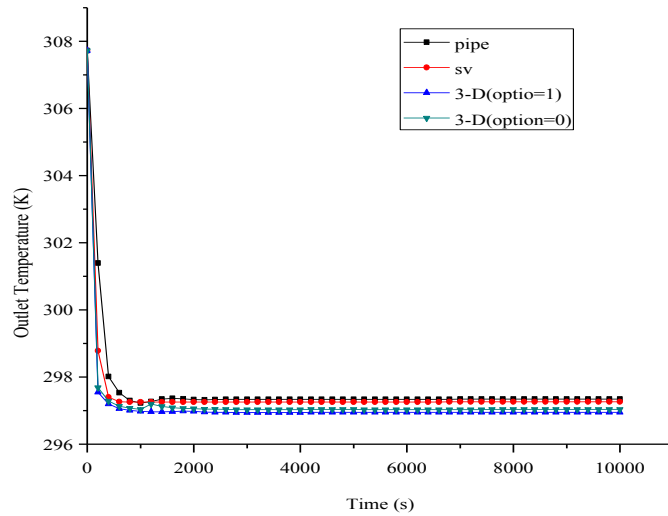


**Figure 25.** Pipe Outlet Temperature

## 2.4 Comparison Between RELAP5-3D and Experimental Results

As described in the paper, there are cold and hot manifold that connect risers and water tank located at the top of cavity. There are three inlets for each manifold: two inlets on each side of the manifold and the other one located at the center of the manifold. In the experiment, the configuration selected for the experiment activity is: side water inlet at the supply manifold and side water outlet at the return manifolds (at the opposite side of the side water inlet). The nodalization is shown in Figure 26.

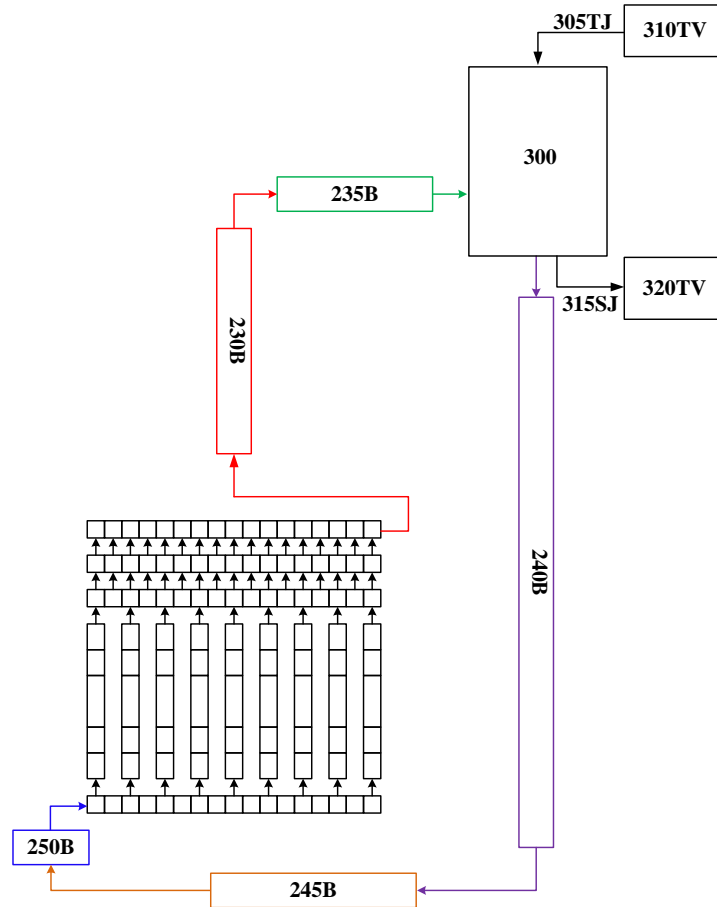


**Figure 26.** Nodalization for Experiment Configuration

Also in the experiment, there is an ice tank, which is the ultimate heat sink in the system. There are 10 ice batches with total amount of ice equal to 27kg[10]. The ice batch was poured into the ice tank when the coolant outlet temperature was high, which will cause a sudden decrease in coolant inlet temperature, as shown in Figure 27.

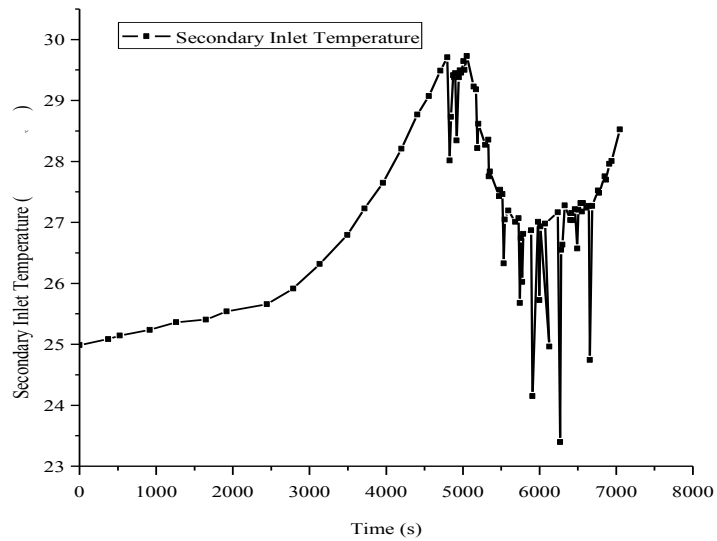


**Figure 27.** Secondary Coolant Inlet Temperature in Experiment

According to the ice batches behavior in the experiment, in RELAP5-3D simulation, the behavior of coolant inlet temperature is replicated, as shown in Figure 28. From the figure, we can see the coolant inlet temperature in RELAP5-3D is almost the same with the temperature behavior in the experiment.

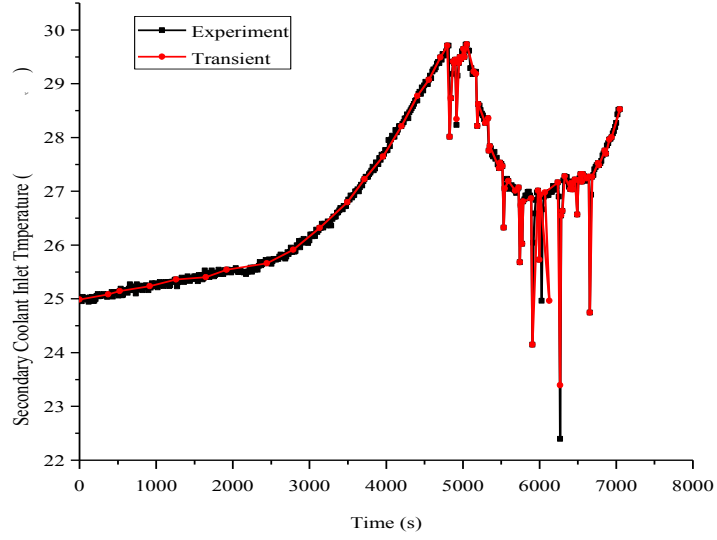


**Figure 28.** Comparison Between Experiment and RELAP5

In RELAP5-3D simulation, I tried to reproduce the power distribution over time, which is added to the vessel, and by comparing the difference between experimental data with simulation results in cavity inlet and outlet temperature as well as the primary loop mass flow rate. In the experiment, the initial power level is 0 and the final power level is 6000W. Finally, the power distribution is shown in Figure 29.

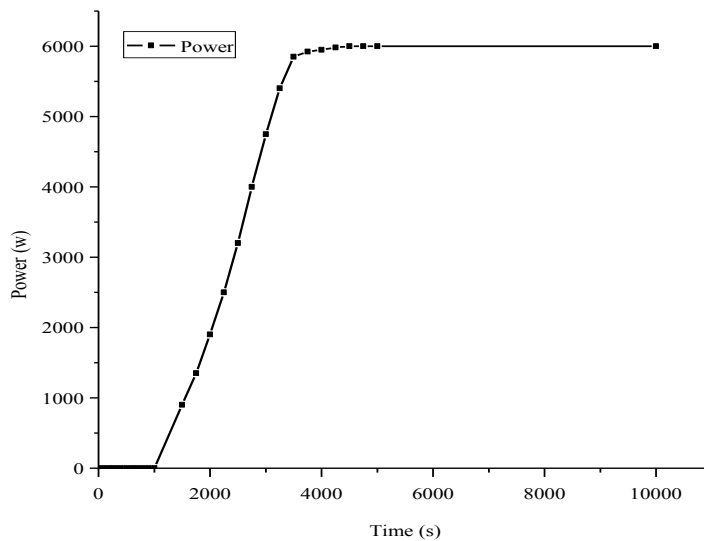


**Figure 29.** Power Distribution Over Time (Vessel)

With the power shown in Figure 29 and the secondary loop inlet temperature shown in Figure 28, the cavity inlet, outlet temperature and mass flow rate is calculated with RELAP5-3D, and also the comparison between RELAP5-3D and experimental results are compared. Figure 30, Figure 31 and Figure 32 show the perfect match between simulation results and experiment data. The power added to pipes increases steadily after 1000s, and the system takes time to reach natural circulation. Before fully natural circulation, cavity inlet and outlet temperature shows slightly difference. Figure 31 gives the cavity inlet temperature and before 2000s, the temperature remains at 297.45 K (24.3°C) and then the temperature increases steadily. There is a good match between experimental and simulation data. In the Figure 30, the cavity outlet temperature shows the similar trend. Compared to experimental results, simulation doesn't show a sharp increase at the beginning, instead it increases a little bit due to the heat added to the pipes and then increases steadily as cavity inlet temperature.

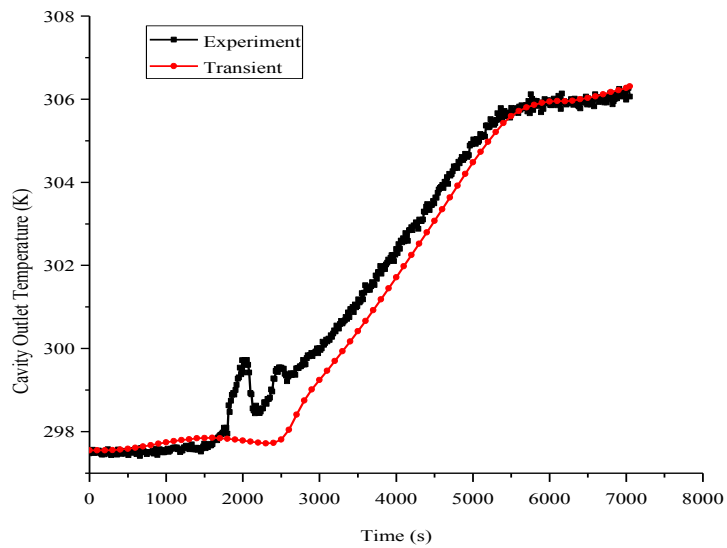


**Figure 30.** Cavity Outlet Temperature

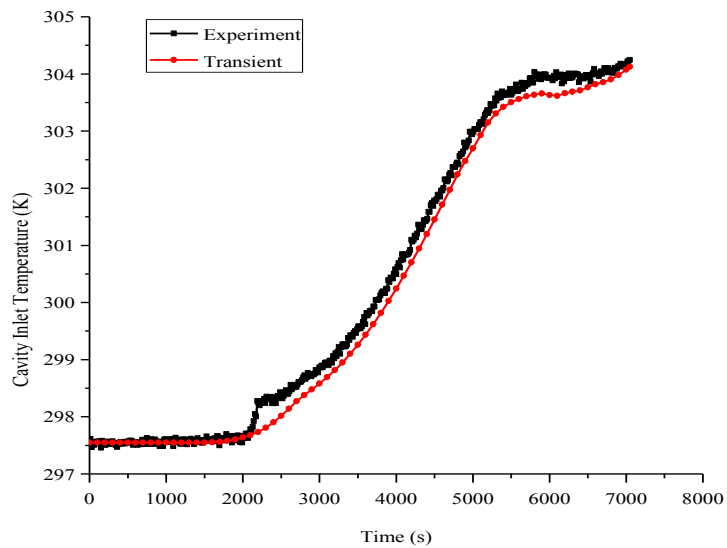


**Figure 31.** Cavity Inlet Temperature

Figure 32 gives the behavior of primary mass flow rate. In RELAP5-3D simulation, at the beginning, inverse flow happens in the system. As Figure 29 shows, the power added to pipe heat structures is 0 before 1000s, so in the system, the only driven force for

natural circulation is gravity, however, considering the friction loss during the flow path, this potential is not enough for coolant flow through the pipes. After 1000s, coolant is heated by power added to pipe heat structures and buoyance caused by coolant density difference helps to terminate inverse flow. Finally gradually natural circulation is buildup and after that, mass flow rate increases steadily until reaches constant.

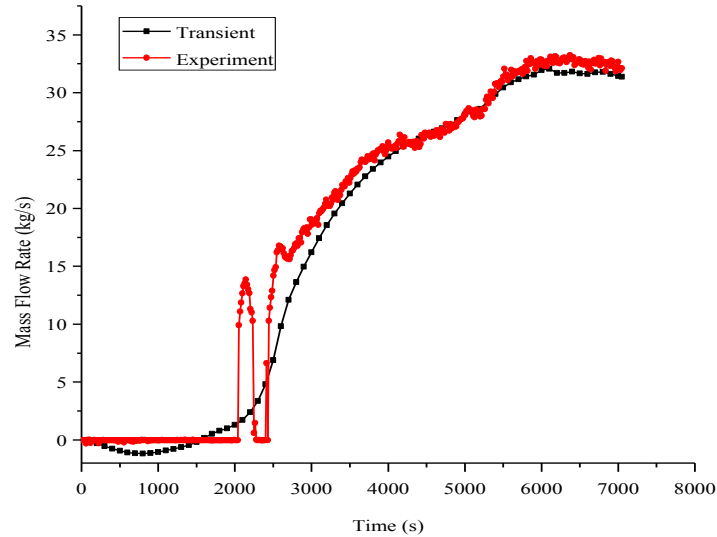


**Figure 32.** Primary Loop Mass Flow Rate

## 2.5 Conclusion

In RELAP5 simulation, we expect the RELAP5-3D model of the experimental facility can accurately reflect the actual facility behavior as best as possible by comparing the simulation results with the experimental data. From the comparisons in the above section, it clearly shows that the RELAP5-3D simulation results match the experimental results very well. So it can be concluded that RELAP5-3D can be applied to HTGR thermal-dynamic behavior analysis in the future.

## 3 GENERATION OF VIEW FACTORS

### 3.1 Introduction

Previous chapters discussed the details of the RCCS experimental facility at Texas A&M University. At this experimental facility, there are three electric heaters installed inside of the experimental vessel, and the heaters are mounted on an independent steel structure thermally insulated from the main facility structure to minimize the heat loss by conduction. Heat transfer in the system can be described as following. Heat is transferred from the vessel to nine risers and fin by radiation and also by natural convection through the air inside the cavity, and the heat transferred to the fin is then transferred by conduction to the risers. Finally, all heat will be transferred to the coolant inside the pipes by convection, if heat loss is neglected. In RELAP5-3D, only one closure can be applied to the heat structure, so the previous experimental works found that radiation heat transfer is predominant in the system and 80% of the heat is transferred to the risers by radiation. In the former RELAP5-3D models, the pipes were assumed to be at the same temperature level in axial direction. However, in the experiment, there is a temperature gradient in the axial direction and there are five thermocouples that are used to monitor the temperature in different axial positions.

### 3.2 Methods of View Factor Calculation

View factor, defined as the fraction of the radiation emission from surface 1 that is intercepted by surface 2, is essential for the evaluation of radiative heat transfer. The most direct way to calculate the view factor, for each surface, is by integration, known as view factor integral. To derive a general expression for the view factor, two arbitrarily oriented surfaces  $A_i$  and  $A_j$  are considered (as shown in Figure 33) with the elemental surface areas —designated as  $dA_i$  and  $dA_j$  respectively.

So the view factors are defined as that given in equation (1).

$$dF_{ij} = \frac{\cos\theta_i \cos\theta_j}{\pi R_{ij}^2} dA_j \quad (1)$$

Where,  $\theta_i$ ,  $\theta_j$  are the angles between the unit normal to the surfaces,  $A_i$  and  $A_j$ , and the length,  $R_{ij}$  is the line connecting the two surfaces. By integrating  $dA_i$  and  $dA_j$  over the whole surface areas,  $A_i$  and  $A_j$ , the view factor can be determined using equation (2).

$$F_{ij} = \frac{1}{A_i} \int_{A_i} \int_{A_j} \frac{\cos\theta_i \cos\theta_j}{\pi R_{ij}^2} dA_i dA_j \quad (2)$$

Where,  $F_{ij}$  is defined as the fraction of the radiation that is emitted from surface  $A_j$  and is intercepted by  $A_i$ , which is given by equation (3)[11].

$$F_{ji} = \frac{1}{A_j} \int_{A_i} \int_{A_j} \frac{\cos\theta_i \cos\theta_j}{\pi R_{ij}^2} dA_i dA_j \quad (3)$$

From the equations (2) and (3), a very important reciprocity relation for view factors always holds:

$$A_i F_{ij} = A_j F_{ji} \quad (4)$$

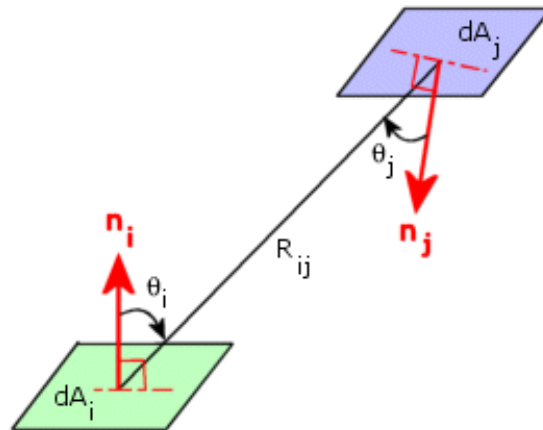


**Figure 33.** View Factors Between Surfaces of Area  $dA_i$  and  $dA_j$  [12]

Also, it is very important to know that the relation is applicable for the additive nature of view factors for a subdivided surface. Considering radiation emission from surface  $i$  to

surface  $j$ , which is divided into  $n$  parts, the additive nature of the view factor relation can be expressed as per equation (5):

$$F_{i(j)} = \sum_{k=1}^n F_{ik} \quad (5)$$

For simple two-dimensional and three-dimensional geometries, the correlations for view factors are presented in the literature [9]. However, in many cases, the arrangement of surfaces and shapes are not so regular and it is difficult to find an appropriate correlation to calculate view factors. For such cases, it is necessary to use numerical methods, such as direct integration, Finite Volume Method, Monte Carlo method, ray tracing method or a combination of these methods.

Finite-Volume Method (FVM) can be applied to various problems including various coordinates (Cartesian coordinate[13, 14], cylindrical coordinate[15, 16]). In calculating view factors with FVM, the surface can be divided into a finite number of discrete non-overlapping control surfaces, then the view factors between control volume surfaces reduces to the calculation of heat transferred from a small concentrated source to another small area [17]. However, for two small targets, it is complicated to compute view factors.

Numerical integration can be used to calculate view factors for both 2D and 3D surfaces. There are many kinds of integration methods that can be applied, such as contour integral, double contour integral, etc.[18].

Monte Carlo (MC) Method is a numerical technique based on statistical characteristics of physical processes, or of analogous models that simulate physical process[19]. The MC method is a kind of stochastic technique, which uses random numbers to simulate the radiation transport, and probability density functions associated with the physical processes of radiation transport.

Among all these methods, MC Method is more suitable for finding the values of view factors because it is able to incorporate all the important effects in a radiation transfer simulation without approximations. MC method has some disadvantages. One is the

requirement of computer time; large amount of time is needed for an acceptable statistical convergence before the predicted results can be considered reliable.

In this thesis work, Monte Carlo N-Particle (MCNP) radiation transport code is employed to calculate the view factors. MCNP is developed to analyze the transport of neutron, photon, electron, or coupled neutron/photon/electron by Monte Carlo method[20]. The code treats an arbitrary three-dimensional configuration of materials in geometric cells bounded by first- and second- degree surfaces and fourth-degree elliptical tori. The other feature that makes MCNP very attracting is its powerful source definition ability and flexible tally structure. In MCNP, there are four possible source types: the first one is fixed source defined by SDEF card, the second one is MCNP generated surface source defined by SSW and SSR card, the third one is Criticality Source defined by KCODE card, the forth one is the user supplied source. Besides this, Card SI (source information), SP (source probability), SB (source bias) and DS (dependent source) cards can also be used with any of the four sources, which make it possible for MCNP to define sources of various types and geometries. Moreover, MCNP can automatically generate summary information which can give a complete accounting of the creation and loss of all tracks and their energy, the number of tracks entering and reentering a cell as well as the track information in the cell, the number of collision in a cell, the average weight, mean free path, the energy of tracks in a cell, the activity of each nuclide in a cell, and a complete weight balance for each cell. In order to accomplish this, MCNP provides seven standard tally types, including F1 (surface current), F2 (surface flux), F4 (track length estimate of cell flux), F5a (flux at a point or ring detector), F6 (track length estimate of energy deposition), F7 (track length estimate of fission energy deposition), F8 (pulse height tally).

### **3.3 Validation of View Factor Calculation using MCNP**

In order to test the ability of MCNP in calculating View Factor, a simple geometry is setup in MCNP, as shown in Fig. 34 and Fig.35. In the two Figures, the length of the cylinder is 1000cm, and radius of the two cylinders are the same( $R=2\text{cm}$ ), so the two

cylinders can be regarded as infinite in Z direction. The shadowed area in Figure 34 and Figure 35 are the source surface.

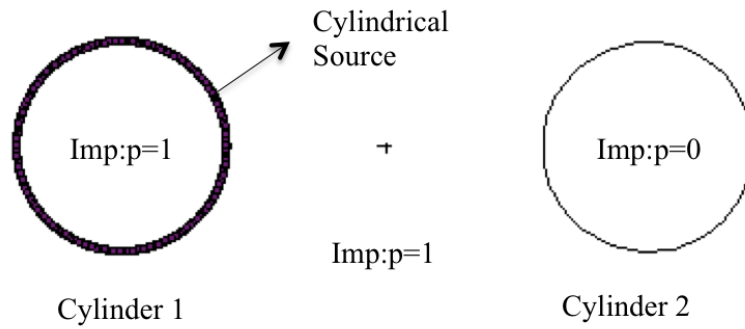


**Figure 34.** xy Plane View of The Example

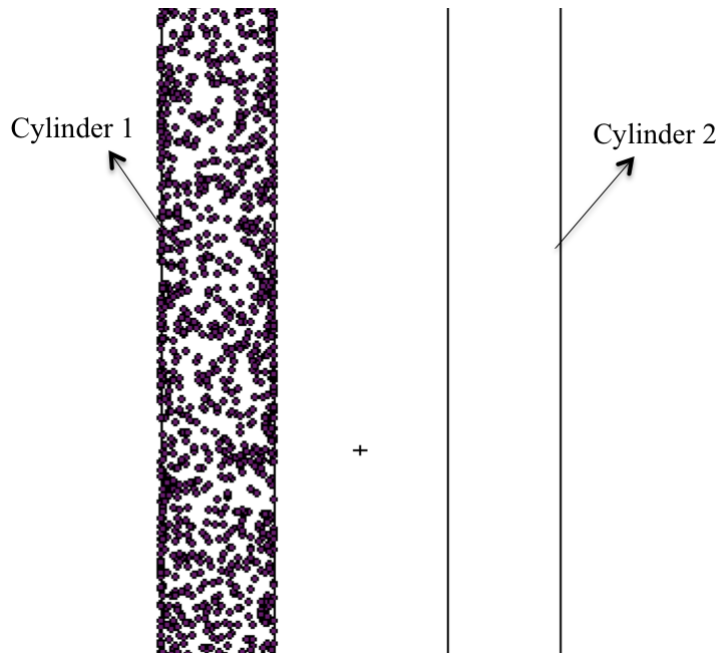


**Figure 35.** xz Plane View of The Example

The formula to calculate view factor between two infinite cylinders are shown below [9]. And the geometry for the formula is shown in Figure 36 and Figure 37. H is infinite in the geometry and  $L > 2R$ .

$$F_{12} = \frac{\sqrt{h^2-4}-h+2\arcsin\frac{2}{h}}{2\pi} \quad (6)$$

Where  $h=L/R$ .

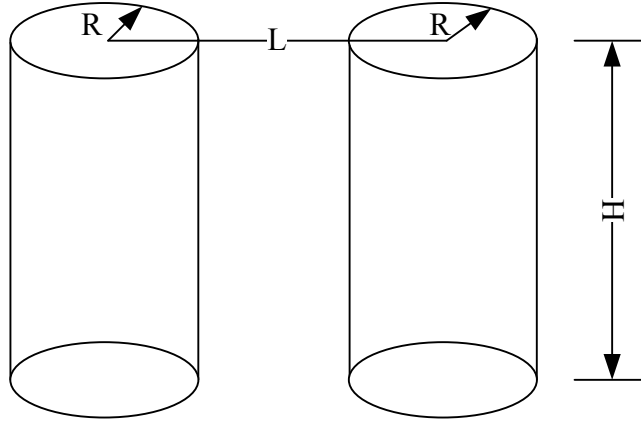


**Figure 36.** Geometry of Two Infinite Cylinders (3D)

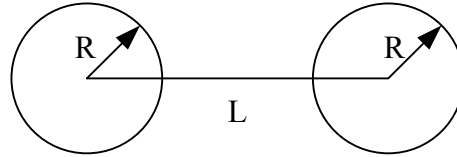


**Figure 37.** Geometry of Two Infinite Cylinders (XY plane)

In the example,  $L=10\text{cm}$ ,  $H=1000\text{cm}$ ,  $R=2\text{cm}$ , so from the formula,  $F_{12} = 0.06455474$ . While from MCNP,  $F_{12} = 0.0645163$ . The difference between the two results is  $0.0000411$ , which is very small compared to the view factor value. So MCNP can be used in calculate view factors and cylindrical surface sources defined in MCNP is reasonable.

### 3.4 Setup of MCNP Model

The geometry of the experimental RCCS facility was modeled using MCNP for the dimensions of the facility discussed in previous chapters, and the model is shown in Figure 34. In the model, pipe 1 to pipe 9 is represented by cylindrical cells in MCNP and they are connected by a plane surface, which represent the fin connection between the

pipes of the experiment facility. All pipes are divided into five parts, shown as “a, b, c, d, and e” and fin surfaces are also divided into 5 parts, named as “al, ar, bl, br, cl, cr, dl, dr, el, er”, in which “l” represents the fin surface on the left side of the corresponding pipe, and “r” represents the fin surface located on the right side of the pipe.

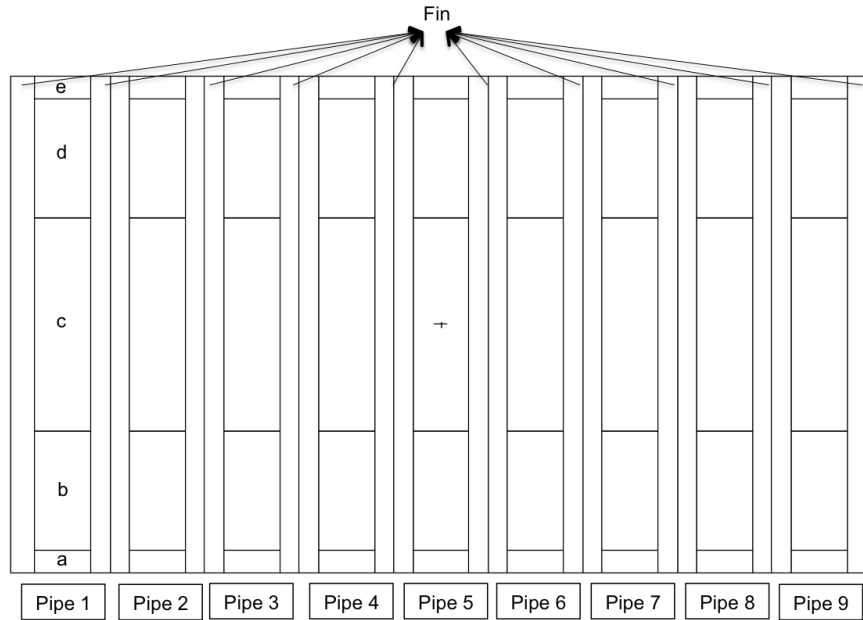


**Figure 38.** XZ Plane View in MCNP Model

In MCNP cases, we treated “a”, “al”, “ar” as a unit. Figure 35 shows an example with pipe1 and its corresponding left and right fin. In MCNP results processing, a, al, ar are treated as a section, so as to “b, bl, br”, “c, cl, cr”, “d, dl, dr”, “e, el, er”. For pipe1, there are totally 5 sections.

el	e	er
dl	d	dr
cl	c	cr
bl	b	br
al	a	ar

**Pipe 1**

**Figure 39.** An Example of Pipe 1 Partition

In MCNP, in order to make sure no radiation particles are lost outside the system, the whole structure is enclosed in a box with length 92.44 cm, width 26.9625 cm and height 110.15cm. Back and front cavity is the space between the pipe and the box boundary. Moreover, the back surface of the box boundary is regarded as the reactor vessel (as shown in Figure 36). The coordinates are also shown in Figure 36. In MCNP problem, particle importance inside the back cavity is 1 and inside front cavity is set to be 0. So, particles are terminated once they pass through the fin surface to the front cavity.

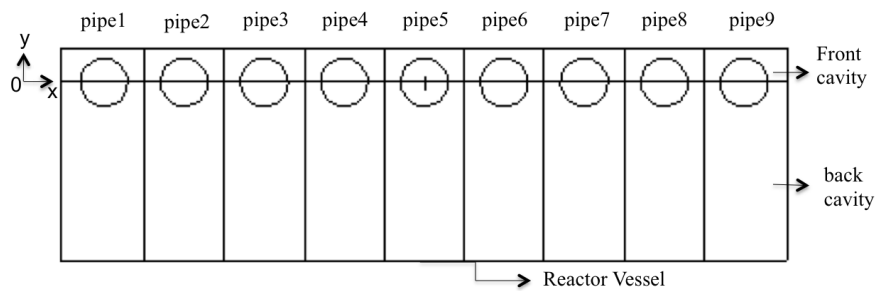


**Figure 40.** XY Plane View in MCNP Model

As per discussions above, the view factor is the fraction of heat radiation released from surface 1 which is intercepted by surface 2. There are totally 55 sections in this problem and the view factors between all 55 sections are supposed to be calculated. What is most important is that each of the 45 sections include two plane surfaces and half of cylindrical surface, which brings out two problems: the first one is how to define the radiation source emitted by one section, and the second one is how to calculate number of particles, which are intercepted by these 45 sections. Actually, the second problem is easy to solve by just tallying three parts of each section separately. For the first problem, unfortunately MCNP cannot define two different types of source (plane surface source and cylindrical surface source) at the same time, so we need to define two types of sources in two separate cases and then combine them together with some factors (in this thesis it is defined as area factor) and the definition of area factor is made later.

MCNP is very powerful in defining all kinds of sources. In this problem, generally, there are two source types, one is surface source, which is very easy to define in MCNP by combination of SDEF card, SIn and SPn; the other one, which is difficult to define, is cylindrical surface source. In MCNP, there is no direct way to define cylindrical source. Cylindrical source in MCNP must be specified as degenerate volume sources, where two equal inner and outer radii are specified on the RAD card using an additional SIn card.

As mentioned above, there are 8 tallies in MCNP that gives users all kinds of information about particles simulated. In this thesis work, F1 tally (surface current) is used because it purely record number of particles passing through certain surface. However, in MCNP output file, tally result is normalized to 1 source particle. Due to the limitation of MCNP, we defined plane surface source and cylindrical surface source separately and each case gives a F1 tally result with corresponding source definition, which is normalized to 1 particle source. So, it is important to process the same number of particles in both cases, and also the area of the source surface also matters in this problem. So, area factor is also calculated based on source surface areas. For the plane surface source, the surface area is  $(46.22-43.65625+37.62375-35.56)*\text{height}$ , while the area of cylindrical surface source is  $\text{height}*\pi*(3.01625+3.01624)/2$ . Then we can get the area factor for plane surface is  $3.281144\text{E}-01$ , while the area factor for cylindrical surface is  $6.718856\text{E}-01$ .

To calculate view factors with MCNP, no material definitions should be used and all cells are defined as void, which enable MCNP to process millions of particles in a short time. Therefore, particles can travel in a straight line without any interaction. In the case of plane surface source, particle importance in the whole system except for the back cavity is 0. So, uniform, isotropic source particles are emitted in one direction, which end passing through the vessel surface and then gets terminated. In the case of cylindrical surface source, the particle importance in the degenerate volume is forced to set to be 1, and the particle importance in other cells is all 0. Finally, F1 tally is set up on the other surfaces other than source surface to count the number of particles that cross the various surfaces.

Another thing that should be pointed out is: in the system, the component surface is not purely plane or purely cylindrical surface, so the view factor from one section to itself is nonzero when the source is the combination of plane surface source and cylindrical surface source, because it is partially concave. However, the summation of all view factors for every section source including the lost should be 1. And the “lost” is all particles which didn’t pass through the surface we are interested.

In MCNP, Monte Carlo statistical uncertainty decreases as particle number increases, and also the tally results should pass 10 statistical checks for the tally fluctuation chart (tfc), including mean behavior, relative error, variance of the variance, figure of merit and the slope. After several tests, 10 billion particles are used to minimize the statistical errors and make sure all checks are passed.

### **3.5 RCCS View Factor Results**

There are three kinds of sources in this problem. The first one is particles are emitted from the reactor vessel. The length of vessel is 92.44 cm, and the vessel is divided into nine parts corresponding to the nine pipes.

And the view factors from one section of the vessel to the other sections are 0, because they are all in the same plane. The view factors from Vessel-1 to the other 63 sections are nonzero. The result of view factors from Vessel-1 is shown in Table 1.

**Table 1.** View Factors of Vessel-1

Vessel-1	P1	P2	P3	P4	P5	P6	P7	P8	P9
<b>Part a</b>	3.65E-03	2.89E-03	1.92E-03	9.65E-04	6.95E-04	5.22E-04	3.73E-04	2.62E-04	1.88E-04
<b>Part b</b>	2.18E-02	2.71E-02	1.78E-02	9.54E-03	4.74E-03	3.42E-03	2.36E-03	1.61E-03	1.14E-03
<b>Part c</b>	5.76E-02	4.57E-02	2.99E-02	1.46E-02	1.03E-02	7.32E-03	4.88E-03	4.30E-03	2.40E-03
<b>Part d</b>	2.73E-02	2.16E-02	1.40E-02	6.77E-03	4.75E-03	3.39E-03	2.32E-03	1.61E-03	1.15E-03
<b>Part e</b>	3.67E-03	2.85E-03	1.96E-03	9.69E-04	7.08E-04	5.34E-04	3.68E-04	2.66E-04	1.91E-04
<b>Lost</b>	6.22E-01								9.94E-01

The other two types of sources should be regarded as a unit. When the source is from fin surfaces, part of the particles will be lost in the pipe (shown in Figure 37). As mentioned above, the united source surface is partially concave, so the lost particles are incorporated into view factor to itself and the method to calculate is shown below.

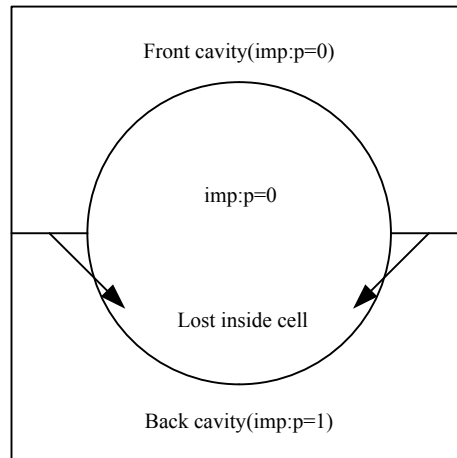


**Figure 41.** Description of Fin Surface Source

When the source is from cylindrical surface, some of the particles are lost inside the pipe (as shown in Figure 38) because cylindrical source is specified as degenerate volume source and some of the particles cross two parts of the fine surfaces in their own unit. In Figure 38, the thickness for the volume source is 0.00001cm, which is the minimum value that can be recognized in MCNP. It also shows four places source particles head (shown in Figure 38 as 1, 2, 3, 4). It is important to know how to deal with particles lost inside the cylindrical cell. From experience, a modification factor was calculated as  $f=1/(\text{fraction of particles lost})$ . Take “pipe1, part a” as an example, 3.4145E-01 is lost, so

the factor is  $f=1/3.4145E-01=1.5185E+00$ . So in this case, all tally results obtained from this cylindrical surface source should be multiplied by this factor.

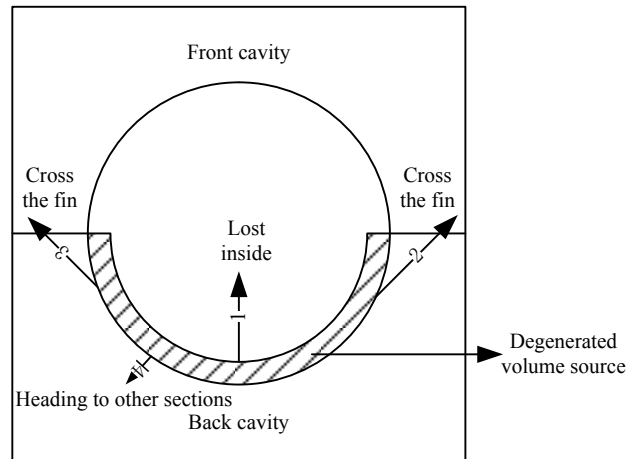


**Figure 42.** Description of Cylindrical Source

Also, it is necessary to calculate view factors from the surface to itself. The method behind this is to use area factor described in section 3.3. From Figure 33 and Figure 34, we can know particles lost through fin surface (in cylindrical surface source) and into the pipe cell (in plane surface source), so we just multiply the value of lost particles with corresponding area factor. The result of the combinations of part “ a ” of “pipe1 and fin 1” is shown in Table 2. From Table 2, it can be noted that the view factor from surface to itself is 0.179198914, and the fraction of lost particles is 0.554561328. The summation of all view factors is 1.000003. The view factor between ‘part a’ of pipe 1 to all sections in pipe3 to pipe 9 is 0 because particles released from the source are blocked on the way to pipe 3-9. The remaining View Factor results are shown in Appendix B.

**Table 2.** View Factor of Part a of pipe 1

	<b>P1</b>	<b>P2</b>	<b>P3, P4, P5, P6, P7, P8, P9</b>
<b>Part a</b>	0.161889171	0.042426475	0
<b>Part b</b>	0.017027825	0.020139713	0
<b>Part c</b>	0.000104248	0.000426133	0
<b>Part d</b>	7.71633E-06	3.13434E-05	0
<b>Part e</b>	9.03421E-07	3.64495E-06	0
<b>v1</b>	0.069299827		
<b>v2</b>	0.051968234		
<b>v3</b>	0.030296225		
<b>v4</b>	0.016578746		
<b>v5</b>	0.009317767		
<b>v6</b>	0.004941522		
<b>v7</b>	0.003051629		
<b>v8</b>	0.002071556		
<b>v9</b>	0.001539486		
<b>Lost</b>	0.568885186		1.000007351

#### 4 SUMMARY

In this paper, the capability of RELAP5-3D applying for thermodynamic behavior analysis of RCCS is investigated. The RELAP5-3D model is based on the small-scale experimental facility established by department of Nuclear Engineering, Texas A&M University. After setting up the RCCS experimental model with RELAP5-3D, different ways to reach steady state is discussed. And also the model is modified with the experimental procedure. At last, comparison between simulation results and experimental data is done and it shows perfect match, which verifies the capability of RELAP5-3D application in HTGR.

Radiation heat transfer predominates in HTGR and it is very important to know view factors between surfaces in RCCS system. Due to the geometry complexity, MCNP based on Monte Carlo Method is applied in view factor calculation. Also, the RCCS system is symmetric in geometry, so only half of the view factors are calculated. It shows that MCNP is powerful in calculating view factors for irregular and complex geometry. However, due to the large amount of surfaces in this geometry, time needed for the whole calculation is very long.

## REFERENCES

1. Goldberg, S.M., R. Rosner, *Nuclear Reactors: Generation to Generation*. 2011, American Academy of Arts & Sciences. p. 1-10.
2. <http://me1065.wikidot.com/geniv>. *Gen IV Reactors* 2008 [cited 2013 04].
3. Lomperski, S., et al., *Generation IV Nuclear Energy System Initiative. Air-Cooled Option RCCS Studies and NSTF Preparation*. 2012, Technical Information Center Oak Ridge Tennessee.
4. Atomics, G., *Gas-Turbine Modular Helium Reactor(GT-MHR) Conceptual Design Description Report* 1996, U.S. Nuclear Regulatory Commission.
5. Lommers, L., *HTGR Technology Course for the Nuclear Regulatory Commission*. AREVA, 2010: p. 24-27
6. Vaghetto, R., S. Lee, and Y.A. Hassan, *Reactor Cavity Cooling System Facility Shakedown and RELAP5-3D Model Validation*. Proceedings of 20th International Conference on Nuclear Engineering, 2012.
7. R. Vaghetto, S.L., Y. A. Hassan, *Reactor Cavity Cooling System Facility Shakedown and RELAP5-3D Model Validation*, in *Proceedings of the 20th International Conference on Nuclear Engineering*. 2012: Anaheim, California, USA.
8. Schultz, R.R., *RELAP5-3D Code Manual Volume V : User ' s Guidelines*. 2005.
9. R.Vaghetto, H.W., Y.A.Hassan, *Simulation of a Simple RCCS Experiment with RELAP5-3D System Code and Computational Fluid Dynamics Computer Program*, in *The 14th International Topical Meeting on Nuclear Reactor Thermalhydraulics*. 2011: Toronto, Ontario, Canada.
10. R.Vaghetto, Y.A.H., *Analysis of the Steady-State Phase of the Reactor Cavity Cooling System Experimental Facility and Comparison with RELAP5-3D Simulations*, in *The 15th International Topical Meeting on Nuclear Reactor Thermal-hydraulics*. 2013: Pisa, Italy.
11. P.Incropera, F. and D.P. Dewitt, *Fundamentals of Heat and Mass Transfer Fourth Edition*. 4 ed. 2006.

12. Wikipedia. *View factor two differential areas illustration*. 2013 [cited 2013 05]; Available from:  
[http://en.wikipedia.org/wiki/File:View\\_factor\\_two\\_differential\\_areas\\_illustration.svg](http://en.wikipedia.org/wiki/File:View_factor_two_differential_areas_illustration.svg).
13. Raithby, G.D. and E.H. Chui, *A Finite-Volume Method for Predicting Radiation Heat Transfer in Enclosure with Participating Media*. Heat Transfer, 1990. **112**(2): p. 415-423.
14. Chai, J.C., H.S. Lee, and S.V. Patankar, *Finite-Volume Method for Radiation Heat Transfer*. Heat Transfer, 1994. **8**(3): p. 419-425.
15. Chui, E.H., G.D. Raithby, and P.M.J. Hughes, *Prediction of Radiative Transfer in Cylindrical Enclosure with the Finite Volume Method*. Heat Transfer, 1992. **6**(4): p. 605-611.
16. Moder, J.P., et al., *Nonaxisymmetric Radiative Transfer in Cylindrical Enclosures*. Heat Transfer B, 1996. **30**: p. 437-452.
17. J.C.Chai, J.P.Moder, and K.C.Karki, *A Procedure For View Factor Calculation using the Finite-Volume Method*. Numerical Heat Transfer B, 2001. **40**: p. 23-35.
18. Diaconu, B.M., M. Cruceru, and A.T. Gheorghian, *View Factors in a Finite Length Axysymmetric Cylindrical Annulus Enclosure*. Journal of Quantitative Spectroscopy & Radiative Transfer, 2012. **113**: p. 2100-2112.
19. Mirhosseini, M. and A.Saboonchi, *View Factor Calculation Using the Monte Carlo Method for a 3-D Stirp Element to Circular Cylinder*. International Communication in Heat and Mass Transfer, 2011. **38**: p. 821-826.
20. Shultis, J.K., R.E.Faw, *An MCNP Premier*. 2005, Dept. of Mechanical and Nuclear Engineering: Manhattan.

## APPENDIX A

### SOURCE DEFINITION IN MCNP

#### 1) Plane Surface Source

```
C    surface source
MODE P
NPS  10000000000
PHYS:P 100 1 1 0 1
SDEF  SUR=41 POS=D1 X=FPOS D2 Y=0.0 Z=D5 PAR=2
      ERG=2.5 VEC=0 -1 0 DIR=D6
SI1  L -4.048125 0.0 -52.535 +4.048125 0.0 -52.535
SP1   0.5           0.5
DS2  S   3           4
SI3   -5.080   -3.01625
SP3   0   1.0
SI4   +3.01625 +5.080
SP4   0   1.0
SI5   -55.075 -49.995
SP5   0   1.0
SI6   0.0   1.0
SP6   0.0   1.0
```

#### 2) Cylindrical Surface Source

```
C    surface source
MODE P
NPS  10000000000
PHYS:P 100 1 1 0 1
SDEF  POS=-10.160 0 -52.535 AXS=0 0 1 PAR=2
      EXT=D1 ERG=2.5 NRM=+1 RAD=D2 CCC=14
SI1  -2.54   +2.54
SP1   0   1
SI2  +3.01624 +3.01625
SP2  -21   1
```

## APPENDIX B

### VIEW FACTOR RESULTS

**Table 3.** Source Surface of P1-Part b

	<b>P1</b>	<b>P2</b>	<b>P3, P4, P5, P6, P7, P8, P9</b>
<b>Part a</b>	0.004205331	0.004899882	0
<b>Part b</b>	0.195384523	0.066815076	0
<b>Part c</b>	0.004887806	0.007734328	0
<b>Part d</b>	1.55992E-05	6.57131E-05	0
<b>Part e</b>	1.48275E-06	6.33181E-06	0
<b>V1</b>	0.09414274		
<b>V2</b>	0.070716942		
<b>V3</b>	0.040907672		
<b>V4</b>	0.021971687		
<b>V5</b>	0.012046298		
<b>V6</b>	0.004864429		
<b>V7</b>	0.003794194		
<b>V8</b>	0.003789905		
<b>V9</b>	0.001854086		
<b>Lost</b>	0.467556562		1.005660589

**Table 4.** Source Surface of P1-Part c

	<b>P1</b>	<b>P2</b>	<b>P3, P4, P5, P6, P7, P8, P9</b>
<b>Part a</b>	1.50155E-05	4.18169E-05	0
<b>Part b</b>	0.031391751	0.010712189	0
<b>Part c</b>	0.200352462	0.077995042	0
<b>Part d</b>	0.003091102	0.003387247	0
<b>Part e</b>	1.49922E-05	4.17274E-05	0
<b>V1</b>	0.118141393		
<b>V2</b>	0.087828325		
<b>V3</b>	0.04936652		
<b>V4</b>	0.024841958		
<b>V5</b>	0.012081998		
<b>V6</b>	0.004146492		
<b>V7</b>	0.002167478		
<b>V8</b>	0.001429398		
<b>V9</b>	0.001028308		
<b>Lost</b>	0.371903113		0.999978328

**Table 5.** Source Surface of P2-Part a

	<b>P1</b>	<b>P2</b>	<b>P3</b>	<b>P4, P5, P6, P7, P8, P9</b>
<b>Part a</b>	0.053123852	0.15720311	0.044060099	0
<b>Part b</b>	0.027055064	0.01392408	0.020827765	0
<b>Part c</b>	0.000435995	8.67992E-05	0.000435973	0
<b>Part d</b>	3.18561E-05	6.32121E-06	3.19005E-05	0
<b>Part e</b>	3.60538E-06	7.23916E-07	3.28957E-06	0
<b>V1</b>	0.054121849			
<b>V2</b>	0.066253689			
<b>V3</b>	0.05216348			
<b>V4</b>	0.030246382			
<b>V5</b>	0.016966314			
<b>V6</b>	0.00958029			
<b>V7</b>	0.004972956			
<b>V8</b>	0.003057551			
<b>V9</b>	0.002162414			
<b>Lost</b>	0.443705734			1.000461092

**Table 6.** Source Surface of P2-Part2

	<b>P1</b>	<b>P2</b>	<b>P3</b>	<b>P4, P5, P6, P7, P8, P9</b>
<b>Part a</b>	0.00526744	0.003895421	0.005268914	0
<b>Part b</b>	0.082774248	0.194154531	0.069403585	0
<b>Part c</b>	0.007910632	0.004464797	0.007909361	0
<b>Part d</b>	6.66651E-05	1.27347E-05	6.6601E-05	0
<b>Part e</b>	6.42306E-06	1.24181E-06	6.40683E-06	0
<b>V1</b>	0.073623414			
<b>V2</b>	0.089915775			
<b>V3</b>	0.070964463			
<b>V4</b>	0.040842721			
<b>V5</b>	0.022475785			
<b>V6</b>	0.012375498			
<b>V7</b>	0.006269563			
<b>V8</b>	0.003792146			
<b>V9</b>	0.0026401			
<b>Lost</b>	0.295543328			0.999651795

**Table 7.** Source Surface of P2-Part3

	<b>P1</b>	<b>P2</b>	<b>P3</b>	<b>P4, P5, P6, P7, P8, P9</b>
<b>Part a</b>	6.02835E-05	1.06356E-05	6.02451E-05	0
<b>Part b</b>	0.00445351	0.002485606	0.019451452	0
<b>Part c</b>	0.090142351	0.198728322	0.090139375	0
<b>Part d</b>	0.004454575	0.002486243	0.004452766	0
<b>Part e</b>	6.00881E-05	1.0623E-05	6.01268E-05	0
<b>V1</b>	0.085831184			
<b>V2</b>	0.103963239			
<b>V3</b>	0.082704462			
<b>V4</b>	0.048342991			
<b>V5</b>	0.026889565			
<b>V6</b>	0.014807914			
<b>V7</b>	0.007433111			
<b>V8</b>	0.004438383			
<b>V9</b>	0.003044134			
<b>Lost</b>	0.205759911			1.000271095

**Table 8.** Source Surface of P3-Part a

	<b>P1</b>	<b>P2</b>	<b>P3</b>	<b>P4</b>	<b>P5, P6, P7, P8, P9</b>
<b>Part a</b>	0	0.044063157	0.159683888	0.044060099	0
<b>Part b</b>	0	0.02457383	0.01911547	0.020827765	0
<b>Part c</b>	0	0.000435995	8.67992E-05	0.000435973	0
<b>Part d</b>	0	3.18561E-05	6.32121E-06	3.19005E-05	0
<b>Part e</b>	0	3.60538E-06	7.31397E-07	3.65742E-06	0
<b>V1</b>	0.031304269				
<b>V2</b>	0.052165293				
<b>V3</b>	0.066253689				
<b>V4</b>	0.05216348				
<b>V5</b>	0.030246382				
<b>V6</b>	0.016966314				
<b>V7</b>	0.00958029				
<b>V8</b>	0.004972956				
<b>V9</b>	0.003178533				
<b>Lost</b>	0.420300428				1.000492682

**Table 9.** Source Surface of P3-Part b

	<b>P1</b>	<b>P2</b>	<b>P3</b>	<b>P4</b>	<b>P5, P6, P7, P8, P9</b>
<b>Part a</b>	0	0.005294518	0.003900349	0.005240586	0
<b>Part b</b>	0	0.082857888	0.194154689	0.069506445	0
<b>Part c</b>	0	0.007897313	0.004466779	0.00789066	0
<b>Part d</b>	0	6.53958E-05	1.32016E-05	6.83563E-05	0
<b>Part e</b>	0	6.61933E-06	9.0336E-07	1.88076E-05	0
<b>V1</b>	0.042243035				
<b>V2</b>	0.070962644				
<b>V3</b>	0.089923978				
<b>V4</b>	0.070970533				
<b>V5</b>	0.040852729				
<b>V6</b>	0.022475588				
<b>V7</b>	0.012376259				
<b>V8</b>	0.006269946				
<b>V9</b>	0.003940865				
<b>Lost</b>	0.259347052				1.000745141

**Table 10.** Source Surface of P3-Part c

	<b>P1</b>	<b>P2</b>	<b>P3</b>	<b>P4</b>	<b>P5, P6, P7, P8, P9</b>
<b>Part a</b>	0	6.61933E-06	9.0336E-07	1.88076E-05	0
<b>Part b</b>	0	6.53958E-05	1.32016E-05	6.83563E-05	0
<b>Part c</b>	0	0.007897313	0.004466779	0.00789066	0
<b>Part d</b>	0	0.082857888	0.194154689	0.069506445	0
<b>Part e</b>	0	0.005294518	0.003900349	0.005240586	0
<b>V1</b>	0.042243035				
<b>V2</b>	0.070962644				
<b>V3</b>	0.089923978				
<b>V4</b>	0.070970533				
<b>V5</b>	0.040852729				
<b>V6</b>	0.022475588				
<b>V7</b>	0.012376259				
<b>V8</b>	0.006269946				
<b>V9</b>	0.003940865				
<b>Lost</b>	0.259347052				1.000745141

**Table 11.** Source Surface of P4-Part a

	<b>P1</b>	<b>P3</b>	<b>P4</b>	<b>P5</b>	<b>P2, P6, P7, P8, P9</b>
<b>Part a</b>	0	0.044051101	0.159683888	0.044060099	0
<b>Part b</b>	0	0.02457383	0.01392408	0.020827765	0
<b>Part c</b>	0	0.000435995	8.67992E-05	0.000435973	0
<b>Part d</b>	0	3.18561E-05	6.32121E-06	3.20499E-05	0
<b>Part e</b>	0	3.60538E-06	7.31397E-07	3.65742E-06	0
<b>V1</b>	0.017601722				
<b>V2</b>	0.030249676				
<b>V3</b>	0.052165293				
<b>V4</b>	0.066253689				
<b>V5</b>	0.05216348				
<b>V6</b>	0.030246382				
<b>V7</b>	0.016966314				
<b>V8</b>	0.00958029				
<b>V9</b>	0.005155649				
<b>Lost</b>	0.411858322				1.000398569

**Table 12.** Source Surface of P4-Part b

	<b>P1, P2</b>	<b>P3</b>	<b>P4</b>	<b>P5</b>	<b>P2, P6, P7, P8, P9</b>
<b>Part a</b>	0	0.00526744	0.003895421	0.004967029	0
<b>Part b</b>	0	0.082774248	0.194154689	0.069403585	0
<b>Part c</b>	0	0.007910632	0.004464797	0.007909361	0
<b>Part d</b>	0	6.66651E-05	1.27347E-05	6.6601E-05	0
<b>Part e</b>	0	6.42306E-06	1.24181E-06	6.40683E-06	0
<b>V1</b>	0.02330527				
<b>V2</b>	0.040842137				
<b>V3</b>	0.07096691				
<b>V4</b>	0.089915775				
<b>V5</b>	0.070964463				
<b>V6</b>	0.040842721				
<b>V7</b>	0.022475785				
<b>V8</b>	0.012375498				
<b>V9</b>	0.006497755				
<b>Lost</b>	0.241265168				1.000358757

**Table 13.** Source Surface of P5-Part a

	<b>P1</b>	<b>P4</b>	<b>P5</b>	<b>P6</b>	<b>P2, P3, P7, P8, P9</b>
<b>Part a</b>	0	0.044063157	0.159683888	0.044060099	0
<b>Part b</b>	0	0.02457383	0.01911547	0.020827765	0
<b>Part c</b>	0	0.000435995	8.67992E-05	0.000435973	0
<b>Part d</b>	0	3.18561E-05	6.32121E-06	3.19005E-05	0
<b>Part e</b>	0	3.60538E-06	7.31397E-07	3.65742E-06	0
<b>V1</b>	0.009906217				
<b>V2</b>	0.016966625				
<b>V3</b>	0.030249676				
<b>V4</b>	0.052165293				
<b>V5</b>	0.066253689				
<b>V6</b>	0.05216348				
<b>V7</b>	0.030246382				
<b>V8</b>	0.016966314				
<b>V9</b>	0.009906437				
<b>Lost</b>	0.402308581				1.000493744

**Table 14.** Source Surface of P5-Part b

	<b>P1, P2, P3</b>	<b>P4</b>	<b>P5</b>	<b>P6</b>	<b>P7, P8, P9</b>
<b>Part a</b>	0	0.044063157	0.01911547	0.044060099	0
<b>Part b</b>	0	0.02457383	0.159683888	0.020827765	0
<b>Part c</b>	0	0.000435995	8.67992E-05	0.000435973	0
<b>Part d</b>	0	3.18561E-05	6.32121E-06	3.19005E-05	0
<b>Part e</b>	0	3.60538E-06	7.31397E-07	3.65742E-06	0
<b>V1</b>	0.010618511				
<b>V2</b>	0.018754061				
<b>V3</b>	0.034103708				
<b>V4</b>	0.059848846				
<b>V5</b>	0.076416212				
<b>V6</b>	0.059846016				
<b>V7</b>	0.034100479				
<b>V8</b>	0.018753422				
<b>V9</b>	0.010618918				
<b>Lost</b>	0.364325938				1.00074716

**Table 15.** Source Surface of P5-Part c

	<b>P1, P2, P3</b>	<b>P4</b>	<b>P5</b>	<b>P6</b>	<b>P7, P8, P9</b>
<b>Part a</b>	0	6.02835E-05	5.90305E-06	5.09749E-05	0
<b>Part b</b>	0	0.00445351	0.001421059	0.003547255	0
<b>Part c</b>	0	0.090142351	0.198696823	0.064750244	0
<b>Part d</b>	0	0.004424665	0.001421692	0.003546406	0
<b>Part e</b>	0	6.01247E-05	5.89301E-06	5.08938E-05	0
<b>V1</b>	0.01530293				
<b>V2</b>	0.026889405				
<b>V3</b>	0.048341142				
<b>V4</b>	0.082706987				
<b>V5</b>	0.103963239				
<b>V6</b>	0.082704462				
<b>V7</b>	0.048342991				
<b>V8</b>	0.026889565				
<b>V9</b>	0.015302185				
<b>Lost</b>	0.176715078				0.99979606

**Table 16.** Source Surface of P6-Part a

	<b>P1, P2, P3, P4</b>	<b>P5</b>	<b>P6</b>	<b>P7</b>	<b>P8, P9</b>
<b>Part a</b>	0	0.044060099	0.159683888	0.044051101	0
<b>Part b</b>	0	0.020827765	0.01392408	0.02457383	0
<b>Part c</b>	0	0.000435973	8.67992E-05	0.000435995	0
<b>Part d</b>	0	3.20499E-05	6.32121E-06	3.18561E-05	0
<b>Part e</b>	0	3.65742E-06	7.31397E-07	3.60538E-06	0
<b>V1</b>	0.005155649				
<b>V2</b>	0.00958029				
<b>V3</b>	0.016966314				
<b>V4</b>	0.030246382				
<b>V5</b>	0.05216348				
<b>V6</b>	0.066253689				
<b>V7</b>	0.052165293				
<b>V8</b>	0.030249676				
<b>V9</b>	0.017601722				
<b>Lost</b>	0.411858322				1.000398569

**Table 17.** Source Surface of P6-Part b

	<b>P1, P2, P3, P4</b>	<b>P5</b>	<b>P6</b>	<b>P7</b>	<b>P8, P9</b>
<b>Part a</b>	0	0.004967029	0.003895421	0.00526744	0
<b>Part b</b>	0	0.069403585	0.194154689	0.082774248	0
<b>Part c</b>	0	0.007909361	0.004464797	0.007910632	0
<b>Part d</b>	0	6.6601E-05	1.27347E-05	6.66651E-05	0
<b>Part e</b>	0	6.40683E-06	1.24181E-06	6.42306E-06	0
<b>V1</b>	0.006497755				
<b>V2</b>	0.012375498				
<b>V3</b>	0.022475785				
<b>V4</b>	0.040842721				
<b>V5</b>	0.070964463				
<b>V6</b>	0.089915775				
<b>V7</b>	0.07096691				
<b>V8</b>	0.040842137				
<b>V9</b>	0.02330527				
<b>Lost</b>	0.241265168				1.000358757

**Table 18.** Source Surface of P7-Part a

	<b>P1, P2, P3, P4, P5</b>	<b>P6</b>	<b>P7</b>	<b>P8</b>	<b>P9</b>
<b>Part a</b>	0	0.044060099	0.159683888	0.044063157	0
<b>Part b</b>	0	0.020827765	0.01911547	0.02457383	0
<b>Part c</b>	0	0.000435973	8.67992E-05	0.000435995	0
<b>Part d</b>	0	3.19005E-05	6.32121E-06	3.18561E-05	0
<b>Part e</b>	0	3.65742E-06	7.31397E-07	3.60538E-06	0
<b>V1</b>	0.003178533				
<b>V2</b>	0.004972956				
<b>V3</b>	0.00958029				
<b>V4</b>	0.016966314				
<b>V5</b>	0.030246382				
<b>V6</b>	0.05216348				
<b>V7</b>	0.066253689				
<b>V8</b>	0.052165293				
<b>V9</b>	0.031304269				
<b>Lost</b>	0.420300428				1.000492682

**Table 19.** Source Surface of P7-Part b

	<b>P1, P2, P3, P4, P5</b>	<b>P6</b>	<b>P7</b>	<b>P8</b>	<b>P9</b>
<b>Part a</b>	0	0.005240586	0.003900349	0.005294518	0
<b>Part b</b>	0	0.069506445	0.194154689	0.082857888	0
<b>Part c</b>	0	0.00789066	0.004466779	0.007897313	0
<b>Part d</b>	0	6.83563E-05	1.32016E-05	6.53958E-05	0
<b>Part e</b>	0	1.88076E-05	9.0336E-07	6.61933E-06	0
<b>V1</b>	0.003940865				
<b>V2</b>	0.006269946				
<b>V3</b>	0.012376259				
<b>V4</b>	0.022475588				
<b>V5</b>	0.040852729				
<b>V6</b>	0.070970533				
<b>V7</b>	0.089923978				
<b>V8</b>	0.070962644				
<b>V9</b>	0.042243035				
<b>Lost</b>	0.259347052				1.000745141

**Table 20.** Source Surface of P7-Part c

	<b>P1, P2, P3, P4, P5</b>	<b>P6</b>	<b>P7</b>	<b>P8</b>	<b>P9</b>
<b>Part a</b>	0	6.02451E-05	1.06356E-05	6.02835E-05	0
<b>Part b</b>	0	0.004453714	0.002485606	0.00445351	0
<b>Part c</b>	0	0.090139375	0.198728322	0.090142351	0
<b>Part d</b>	0	0.004452766	0.002486243	0.004454575	0
<b>Part e</b>	0	6.01268E-05	1.0623E-05	6.00881E-05	0
<b>V1</b>	0.003044134				
<b>V2</b>	0.004438383				
<b>V3</b>	0.007433111				
<b>V4</b>	0.014807914				
<b>V5</b>	0.026889565				
<b>V6</b>	0.048342991				
<b>V7</b>	0.082704462				
<b>V8</b>	0.103963239				
<b>V9</b>	0.085831184				
<b>Lost</b>	0.221281285				1.000794731

**Table 21.** Source Surface of P8-Part a

	<b>P1, P2, P3, P4, P5, P6</b>	<b>P7</b>	<b>P8</b>	<b>P9</b>
<b>Part a</b>	0	0.044060099	0.15720311	0.053123852
<b>Part b</b>	0	0.020827765	0.01392408	0.027055064
<b>Part c</b>	0	0.000435973	8.67992E-05	0.000435995
<b>Part d</b>	0	3.19005E-05	6.32121E-06	3.18561E-05
<b>Part e</b>	0	3.28957E-06	7.23916E-07	3.60538E-06
<b>V1</b>	0.002162414			
<b>V2</b>	0.003057551			
<b>V3</b>	0.004972956			
<b>V4</b>	0.00958029			
<b>V5</b>	0.016966314			
<b>V6</b>	0.030246382			
<b>V7</b>	0.05216348			
<b>V8</b>	0.066253689			
<b>V9</b>	0.054121849			
<b>Lost</b>	0.443705734			1.000461092

**Table 22.** Source Surface of P8-Part b

	<b>P1, P2, P3, P4, P5, P6</b>	<b>P7</b>	<b>P8</b>	<b>P9</b>
<b>Part a</b>	0	0.005268914	0.003895421	0.00526744
<b>Part b</b>	0	0.069403585	0.194154531	0.082774248
<b>Part c</b>	0	0.007909361	0.004464797	0.007910632
<b>Part d</b>	0	6.6601E-05	1.27347E-05	6.66651E-05
<b>Part e</b>	0	6.40683E-06	1.24181E-06	6.42306E-06
<b>V1</b>	0.0026401			
<b>V2</b>	0.003792146			
<b>V3</b>	0.006269563			
<b>V4</b>	0.012375498			
<b>V5</b>	0.022475785			
<b>V6</b>	0.040842721			
<b>V7</b>	0.070964463			
<b>V8</b>	0.089915775			
<b>V9</b>	0.073623414			
<b>Lost</b>	0.295543328			Sum=0.999651795

**Table 23.** Source Surface of P8-Part c

	<b>P1, P2, P3, P4, P5, P6</b>	<b>P7</b>	<b>P8</b>	<b>P9</b>
<b>Part a</b>	0	6.02451E-05	1.06356E-05	6.02835E-05
<b>Part b</b>	0	0.019451452	0.002485606	0.00445351
<b>Part c</b>	0	0.090139375	0.198728322	0.090142351
<b>Part d</b>	0	0.004452766	0.002486243	0.004454575
<b>Part e</b>	0	6.01268E-05	1.0623E-05	6.00881E-05
<b>V1</b>	0.003044134			
<b>V2</b>	0.004438383			
<b>V3</b>	0.007433111			
<b>V4</b>	0.014807914			
<b>V5</b>	0.026889565			
<b>V6</b>	0.048342991			
<b>V7</b>	0.082704462			
<b>V8</b>	0.103963239			
<b>V9</b>	0.085831184			
<b>Lost</b>	0.205759911			Sum=1.000271095

**Table 24.** Source Surface of P9-Part a

	<b>P1, P2, P3, P4, P5, P6, P7</b>	<b>P8</b>	<b>P9</b>
<b>Part a</b>	0	0.042426475	0.161889171
<b>Part b</b>	0	0.020139713	0.017027825
<b>Part c</b>	0	0.000426133	0.000104248
<b>Part d</b>	0	3.13434E-05	7.71633E-06
<b>Part e</b>	0	3.64495E-06	9.03421E-07
<b>V1</b>	0.001539486		
<b>V2</b>	0.002071556		
<b>V3</b>	0.003051629		
<b>V4</b>	0.004941522		
<b>V5</b>	0.009317767		
<b>V6</b>	0.016578746		
<b>V7</b>	0.030296225		
<b>V8</b>	0.051968234		
<b>V9</b>	0.069299827		
<b>Lost</b>	0.568885186		Sum=1.000007351

**Table 25.** Source Surface of P9-Part b

	<b>P1, P2, P3, P4, P5, P6, P7</b>	<b>P8</b>	<b>P9</b>
<b>Part a</b>	0	0.004899882	0.004205331
<b>Part b</b>	0	0.066815076	0.195384523
<b>Part c</b>	0	0.007734328	0.004887806
<b>Part d</b>	0	6.57131E-05	1.55992E-05
<b>Part e</b>	0	6.33181E-06	1.48275E-06
<b>V1</b>	0.001854086		
<b>V2</b>	0.003789905		
<b>V3</b>	0.003794194		
<b>V4</b>	0.004864429		
<b>V5</b>	0.012046298		
<b>V6</b>	0.021971687		
<b>V7</b>	0.040907672		
<b>V8</b>	0.070716942		
<b>V9</b>	0.09414274		
<b>Lost</b>	0.467556562		Sum=1.005660589

**Table 26.** Source Surface of P9-Part c

	<b>P1, P2, P3, P4, P5, P6, P7</b>	<b>P8</b>	<b>P9</b>
<b>Part a</b>	0	4.18169E-05	1.50155E-05
<b>Part b</b>	0	0.010712189	0.031391751
<b>Part c</b>	0	0.077995042	0.200352462
<b>Part d</b>	0	0.003387247	0.003091102
<b>Part e</b>	0	4.17274E-05	1.49922E-05
<b>V1</b>	0.001028308		
<b>V2</b>	0.001429398		
<b>V3</b>	0.002167478		
<b>V4</b>	0.004146492		
<b>V5</b>	0.012081998		
<b>V6</b>	0.024841958		
<b>V7</b>	0.04936652		
<b>V8</b>	0.087828325		
<b>V9</b>	0.118141393		
<b>Lost</b>	0.371903113		Sum=0.999978328